

# A frugal CRISPR kit for equitable and accessible education in gene editing and synthetic biology

Received: 15 October 2023

Accepted: 22 July 2024

Published online: 03 August 2024

 Check for updates

Marvin Collins<sup>1,8</sup>, Matthew B. Lau<sup>2,8</sup>, William Ma<sup>3</sup>, Aidan Shen<sup>4</sup>, Brenda Wang<sup>1</sup>, Sa Cai<sup>5</sup>, Marie La Russa<sup>1</sup>, Michael C. Jewett<sup>1</sup> & Lei S. Qi<sup>1,6,7</sup> ✉

Equitable and accessible education in life sciences, bioengineering, and synthetic biology is crucial for training the next generation of scientists, fostering transparency in public decision-making, and ensuring biotechnology can benefit a wide-ranging population. As a groundbreaking technology for genome engineering, CRISPR has transformed research and therapeutics. However, hands-on exposure to this technology in educational settings remains limited due to the extensive resources required for CRISPR experiments. Here, we develop CRISPRkit, an affordable kit designed for gene editing and regulation in high school education. CRISPRkit eliminates the need for specialized equipment, prioritizes biosafety, and utilizes cost-effective reagents. By integrating CRISPRi gene regulation, colorful chromoproteins, cell-free transcription-translation systems, smartphone-based quantification, and an in-house automated algorithm (CRISPECTRA), our kit offers an inexpensive (~\$2) and user-friendly approach to performing and analyzing CRISPR experiments, without the need for a traditional laboratory setup. Experiments conducted by high school students in classroom settings highlight the kit's utility for reliable CRISPRkit experiments. Furthermore, CRISPRkit provides a modular and expandable platform for genome engineering, and we demonstrate its applications for controlling fluorescent proteins and metabolic pathways such as melanin production. We envision CRISPRkit will facilitate biotechnology education for communities of diverse socioeconomic and geographic backgrounds.

Tools and resources that facilitate accessible K-12 (kindergarten to high school) education in life sciences, bioengineering, and synthetic biology are crucial for fostering a more informed and equitable society<sup>1,2</sup>. Accessible education not only inspires the next generation of scientists but also creates citizens who can comprehend the complex

language behind cutting-edge biotechnologies. This understanding promotes transparency and responsibility in public decision-making while reducing confusion and apprehension. Furthermore, it promotes biotechnology democratization, ensuring that advances in life sciences and bioengineering benefit everyone, regardless of

<sup>1</sup>Department of Bioengineering, Stanford University, Stanford, CA 94305, USA. <sup>2</sup>Program of Biomedical Computation, Stanford University, Stanford, CA 94305, USA. <sup>3</sup>Chinese International School, Hong Kong 999077 Hong Kong SAR, China. <sup>4</sup>East Chapel Hill High School, Chapel Hill, NC 27514, USA.

<sup>5</sup>Department of Materials Science and Engineering, Stanford University, Stanford, CA 94305, USA. <sup>6</sup>Sarafan ChEM-H, Stanford University, Stanford, CA 94305, USA. <sup>7</sup>Chan Zuckerberg Biohub – San Francisco, San Francisco, CA 94158, USA. <sup>8</sup>These authors contributed equally: Marvin Collins, Matthew B. Lau.

✉ e-mail: [slqi@stanford.edu](mailto:slqi@stanford.edu)

socioeconomic background, including individuals with limited technical and financial resources.

Major barriers remain in promoting accessible education on cutting-edge biotechnologies. These barriers stem from the complex nature of these technologies, the need for expensive resources and specialized equipment, and biosafety concerns associated with hands-on experience. Socioeconomic and geographic disparities in access to quality educational resources further compound these challenges. Consequently, education on bioengineering in the K-12 setting has been largely confined to theoretical content presented in classrooms.

CRISPR-Cas gene editing technology has recently revolutionized biomedical research and therapeutics<sup>3–5</sup>. Researchers have demonstrated that CRISPR-based gene therapy can remedy the dysfunction of the oxygen-carrying hemoglobin gene, providing a cure for sickle cell anemia<sup>6,7</sup>. Beyond clinical applications, the technology has enabled researchers to alter the genetic code of various organisms, including animals, plants, and microbes, facilitating advanced genetic engineering that would have been impossible a decade ago<sup>8,9</sup>. Despite its transformative impact on biological sciences at the university and research institute level, hands-on experience with CRISPR technology has been absent from high-school curricula due to the extensive resource requirements for conducting CRISPR experiments (Fig. 1a). Performing CRISPR experiments in living organisms, such as in microbes or mammalian cells, in a classroom setting presents multiple challenges. These include the high cost of equipment and reagents, biosafety requirements for handling living cells and biohazards, and lengthy, complex protocols. These obstacles are often insurmountable for most high schools, leaving students with limited hands-on experience with CRISPR technology.

While previous studies have successfully reduced the requirements for performing CRISPR experiments by using cell-free systems, they still necessitate specialized equipment (e.g., incubators or imagers), expensive apparatus (e.g., pipettes), and complex software for data analysis<sup>10–13</sup>. From an accessibility perspective, we reasoned that eliminating these requirements is crucial to providing hands-on CRISPR experiences to high school students in a more equitable setting (Fig. 1a). Our goal is to develop a frugal kit that eliminates the need for equipment, reduces reagent costs, and minimizes biosafety concerns. Here we present CRISPRkit, an affordable and accessible CRISPR kit designed for gene editing experiments in a classroom setting without equipment requirement. Given that many high school students have access to smartphones, we utilize smartphones to measure CRISPR activity and analyze data using our algorithm termed CRISPR spectra. As an experimental and computational bundle, CRISPRkit is applicable to most high school curricula in low-resource settings and aims to facilitate accessible education on cutting-edge gene-editing technology.

## Results

### The design of a frugal and accessible CRISPR kit for education

We analyzed two potential mechanisms for implementing CRISPR experiments in the educational setting (Fig. 1b). One mechanism is gene editing that uses the nuclease Cas9 for DNA cleavage<sup>14–16</sup>, and the other is gene regulation that uses the nuclease-dead dCas9 for controlling transcription of the target gene, a method termed CRISPR interference (CRISPRi)<sup>17</sup>. Both mechanisms are based on single guide RNA (sgRNA)-directed specific DNA targeting and can generate visualizable outcomes on the genes encoded by the target DNA.

The traditional method of performing CRISPR experiments in living cells necessitates the execution of many costly and time-consuming steps, including transforming competent cells, plating transformed cells, picking colonies, and growing the cells overnight. Our proposed CRISPRkit utilizes a cell-free transcription-translation system, termed cell-free system (CFS), which has been employed for measuring gene expression and CRISPR gene editing<sup>10,18,19</sup> (Fig. 1c). By

using CFS reagents in place of living cells, we eliminate the biosafety and logistical concerns of cell culture, thus improving accessibility. For visible readouts, we adopted chromoproteins, which are pigmented proteins that do not require special light wavelengths or filters to visualize. We chose three chromoproteins with distinct colors that resemble the RGB color mode (red, yellow/green, and blue): eforRed<sup>20</sup>, fwYellow<sup>21</sup>, and aeBlue<sup>22</sup>. Using the *Streptococcus pyogenes* Cas9 system, we designed single guide RNAs (sgRNAs) that specifically target the protein-coding sequence of each chromoprotein to achieve efficient and specific DNA cutting or transcriptional repression.

In the CRISPRkit design, in the absence of Cas9/dCas9 protein or an sgRNA, the transcription and translation machinery produce chromoproteins that appear as visible pigment. When Cas9/dCas9 and a targeting sgRNA are present, they form a ribonucleoprotein complex to cut DNA or repress transcription of the chromoprotein, reducing the intensity of pigmentation. We measure activity of CRISPRkit by quantifying the level of pigmentation change. We also compared two setups: one is termed the ‘high-tech’ setup that uses pipettes for liquid transfer, an incubator for precise temperature control, and a fluorescence plate reader for measurement; the other is termed the ‘low-tech’ setup that relies on inoculation loops for liquid transfer, requires no temperature control, and uses a smartphone for measurement (Fig. 1c, **Methods**).

### Testing the performance of the single-color CRISPRkit in the laboratory setup

We first designed a set of plasmids to express three distinct chromoproteins and a set of plasmids expressing specific sgRNAs for each chromoprotein (Fig. 2a, Supplementary Tables 1–3). There are two options for designing an sgRNA targeting a double-stranded DNA: targeting either the template or the non-template strand. Previous studies have shown that only non-template-targeting sgRNA can repress transcription, due to steric hindrance between dCas9 and the RNA polymerase<sup>17,23</sup> (Supplementary Fig. 1). We therefore designed sgRNAs that target the non-template strand of each chromoprotein, using the CRISPR-ERA algorithm to select sgRNAs without off-target binding sites<sup>24</sup>. We encoded each chromoprotein and each sgRNA under the control of a strong  $\sigma 70$  promoter (J23119) (Fig. 2a, **Methods**).

For experiments, we used pipettes to add Cas9 or dCas9 protein and sgRNA plasmids and incubated each reaction at 28 °C for 24 h in 1.5 mL Eppendorf tubes (Fig. 2b). We quantified fluorescence of eforRed and fwYellow or absorbance of aeBlue using a fluorescence plate reader after transferring samples to a 384-well plate (**Methods**). We chose to measure the absorbance of aeBlue because, unlike eforRed or fwYellow, there is not a suitable fluorescence excitation/emission wavelength that has been found for this protein<sup>22</sup>.

We compared Cas9 (editing) and dCas9 (regulation) side-by-side and tested whether different chromoproteins can be used in the cell-free CRISPRkit experiments and whether they can be specifically targeted by their cognate sgRNAs (Supplementary Fig. 2a). We observed strong chromoprotein expression and visible colors without Cas9 or dCas9 for all three chromoproteins (Fig. 2c, d). In the Cas9 case, we observed significant reduction of eforRed or fwYellow with added sgRNA but not for aeBlue. Notably, adding Cas9 alone (without an sgRNA) significantly reduced the production of chromoproteins, likely suggesting off-target cleavage activity of Cas9 even without a guide (comparing groups PC and NG, Fig. 2c).

In comparison, dCas9 showed little off-target activity and more efficient reduction of chromoprotein pigmentation with cognate sgRNAs (Fig. 2d, e). From the fluorescent plate reader quantification, compared to the no-guide condition (CFS with chromoprotein plasmid and dCas9 only), eforRed and fwYellow CRISPRi showed 126- and 22-fold of repression, respectively (Fig. 2c). The aeBlue CRISPRi showed a smaller fold change (2.1-fold), likely due to the suboptimal

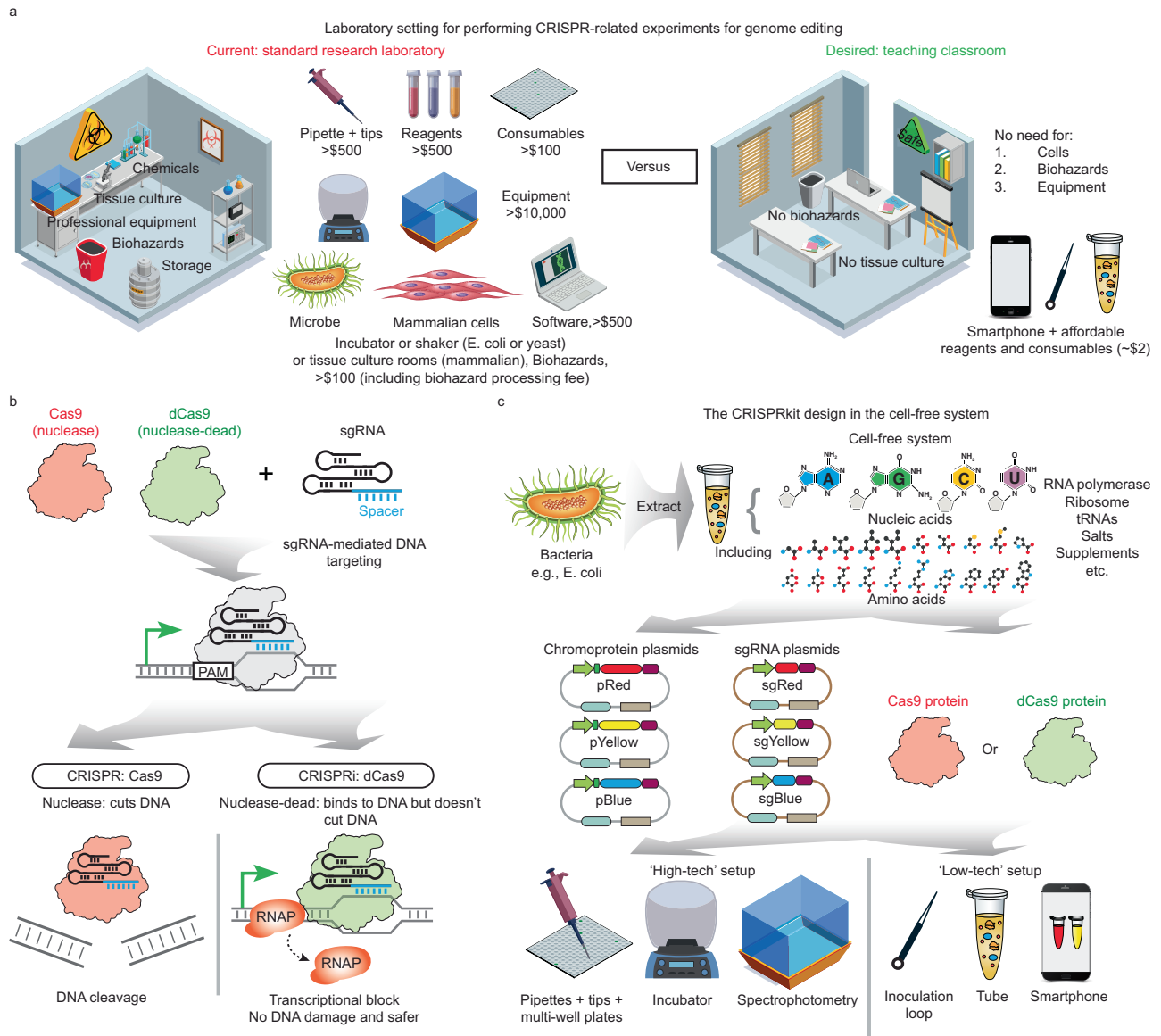


**Fig. 1 | The concept and design of accessible CRISPRkit for high school education.** **a** A comparison between two settings for performing CRISPR experiments. The left shows a laboratory setting. This involves chemicals, tissue culture, biohazards, and equipment such as incubator and fluorescence measurement equipment. A CRISPR experiment requires access to pipettes and pipette tips (>\$500), reagents for molecular cloning and tissue culture (>\$500), consumables such as 384-well plates (>\$100), bacteria or yeast or mammalian cell cultures that require incubator, shaker, or a tissue culture room, biohazards, equipment (>\$10,000), and software (>\$500). The right shows a classroom setting. No cells, biohazards, or professional equipment are needed in this frugal setting. The desired CRISPRkit costs in the range of \$1–2 for reagents and consumables. **b** Illustration of Cas9-mediated genome editing (red) and nuclease-dead dCas9-mediated (green) genome repression (termed CRISPR interference or CRISPRi). Both molecules can bind

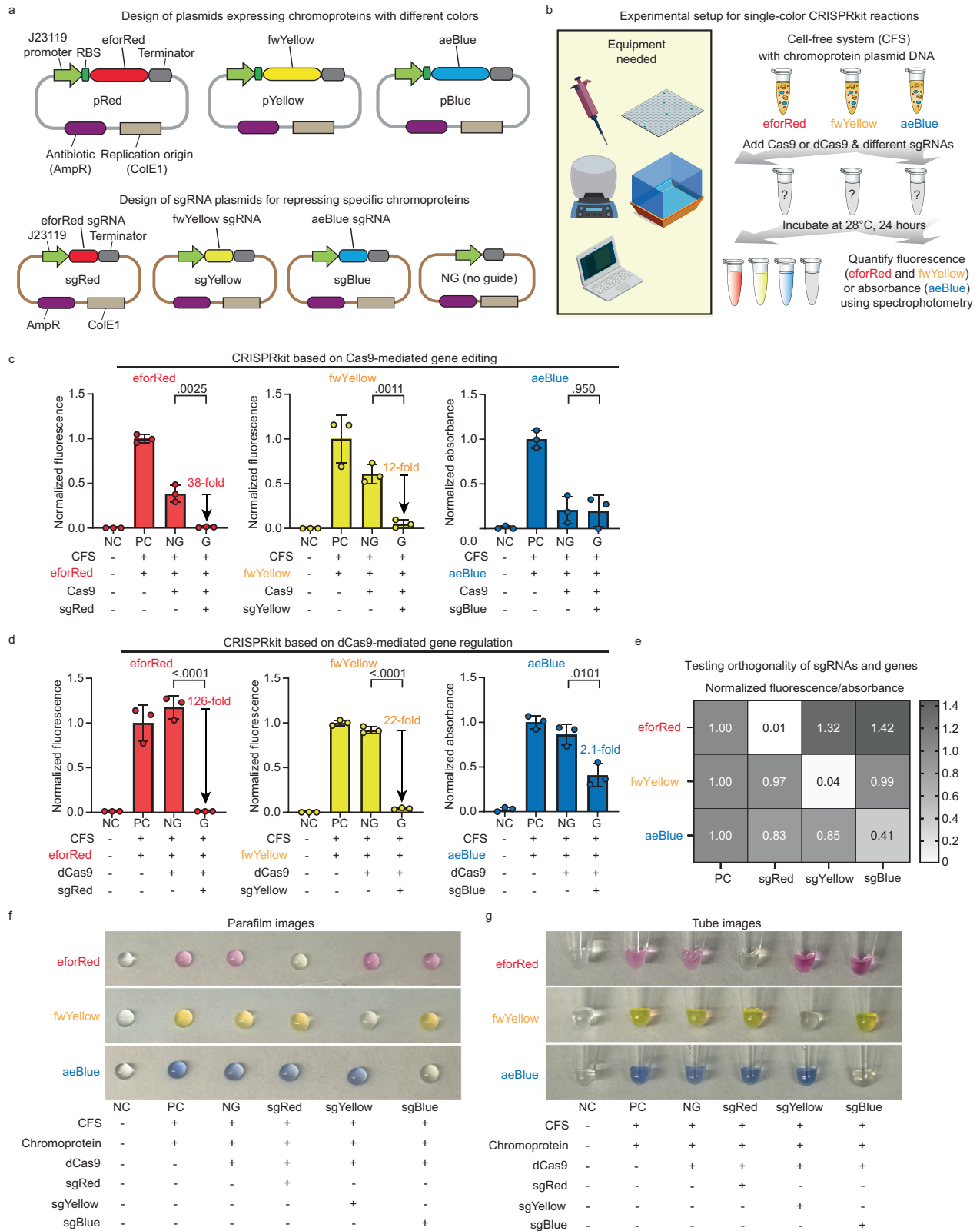
to specific DNA targets via single guide RNA (sgRNA)-mediated RNA-DNA complementarity with a protospacer adjacent motif (PAM). Upon binding to DNA targets, Cas9 cuts DNA into fragments. On the contrary, dCas9 acts as a transcription block to sterically hinder the binding or progression of RNA polymerase (RNAP) on the DNA, repressing transcription of the target gene, without DNA cleavage. **c**. Our design is based on CRISPRi that represses gene expression of the target DNA. The cell-free system (CFS) is mixed with plasmids that encode chromoproteins with various colors (pRed, pYellow, pBlue), plasmids that encode chromoprotein-specific sgRNAs (sgRed, sgYellow, sgBlue), and purified dCas9 protein. We compare two experimental setups, one is termed high-tech involving traditional laboratory equipment such as pipettes, 384-well plates, incubator, and spectrophotometry, and another is termed low-tech involving smartphones, inoculation loops, and tubes.

measurement using absorbance by the plate reader<sup>22</sup>. Yet, visually from parafilm or tube images taken by smartphone, we observed strong pigmentation without CRISPRi and almost no color with CRISPRi (Fig. 2f, g). This suggests that smartphone images might offer a better method to quantify aeBlue pigmentation level that is more consistent with the visual observations. We also confirmed that the sgRNAs acted orthogonally and only repressed their cognate targets (Fig. 2e). We noticed modestly elevated eforRed pigmentation in the presence of sgRNAs targeting feYellow or aeBlue, for reasons unknown (Fig. 2e).

Due to the high leakiness of Cas9, we opted for dCas9 to implement the CRISPRkit design. Our single-color characterization data also suggests that the CFS provides an effective and robust way of performing gene-specific CRISPRi experiments with visible chromoprotein outcomes.

### Testing the performance of dual-color CRISPRkit in the laboratory setup

We next tested whether multiple chromoproteins can be used in the same reaction and whether each gene can be specifically repressed by



their targeting sgRNAs. To achieve this, we used pipettes to mix eforRed and fwYellow plasmids with an equimolar ratio and added dCas9 protein and single or double sgRNA plasmids in 1.5 mL Eppendorf tubes (Fig. 3a, Supplementary Fig. 2b). Like the single-color experiment, we quantified fluorescence of eforRed and fwYellow using the 384-well-based fluorescence plate reader (Methods).

The dual-color CRISPRkit experiment showed that individual chromoprotein genes can be specifically and significantly repressed by their individual sgRNA (Fig. 3b). When both sgRNAs were present, we observed strong and significant repression of both chromoproteins. Both parafilm and tube images taken by smartphone showed visually distinct colors that were consistent with measurement by the



**Fig. 2 | Design, implementation, and characterization of a single-color CRISPRkit under high-tech setup.** **a** Schematic of plasmids encoding chromoproteins (top) and sgRNAs (bottom). Three primary plasmids encode eforRed, fwYellow, and aeBlue, each containing a strong bacterial  $\sigma_{70}$  promoter J23119, a strong ribosome binding site (RBS), codon-optimized coding sequence, and a transcriptional terminator. Each sgRNA plasmid targets a specific chromoprotein gene, also containing a J23119 promoter, the sgRNA-coding sequence, and a transcriptional terminator. **b** High-tech single-color experiment setup using CRISPRkit. The cell-free system is mixed with one chromoprotein plasmid and one sgRNA plasmid per tube. After incubation at 28 °C for 24 h, results are quantified using a fluorescence plate reader. **c** Data showing performance of single-color CRISPRkit reactions using Cas9, measured by a fluorescence plate reader. Four conditions are compared for each chromoprotein: negative control (NC) with water only, positive control (PC) with CFS and chromoprotein plasmid, no-guide condition (NG) with CFS, chromoprotein plasmid, Cas9 protein, and empty sgRNA plasmid, and targeting sgRNA condition (G) with CFS, chromoprotein plasmid, Cas9 protein, and

cognate sgRNA. **d** Data showing performance of single-color CRISPRkit reactions using nuclease-dead dCas9 with a similar setup to Fig. 2c. For **c**, **d**, three biological replicates calculated from the mean of two technical replicates each are plotted for each group. The bars represent the mean and the error bars represent the standard deviation. Unpaired two-sided Student's t-test was performed; p values are indicated above the no guide and guide condition bars. **e** Heatmap showing the orthogonality of sgRNAs for repressing each chromoprotein expression. Normalized fluorescence (for eforRed and fwYellow) and absorbance (for aeBlue) to positive controls (PC) are shown. **f**, **g** Smartphone images of the single-color CRISPRkit reactions transferred to a parafilm (**f**) or 0.6 mL PCR tubes (**g**), after incubation at 28 °C for 24 h. From left to right, each group represent negative control (NC), positive control (PC, CFS + chromoprotein plasmid), no-guide (NG, CFS + chromoprotein plasmid + dCas9 protein + empty sgRNA plasmid), and targeting sgRNA for eforRed (sgRed), fwYellow (sgYellow), and aeBlue (sgBlue). Source data are provided as a Source Data file.

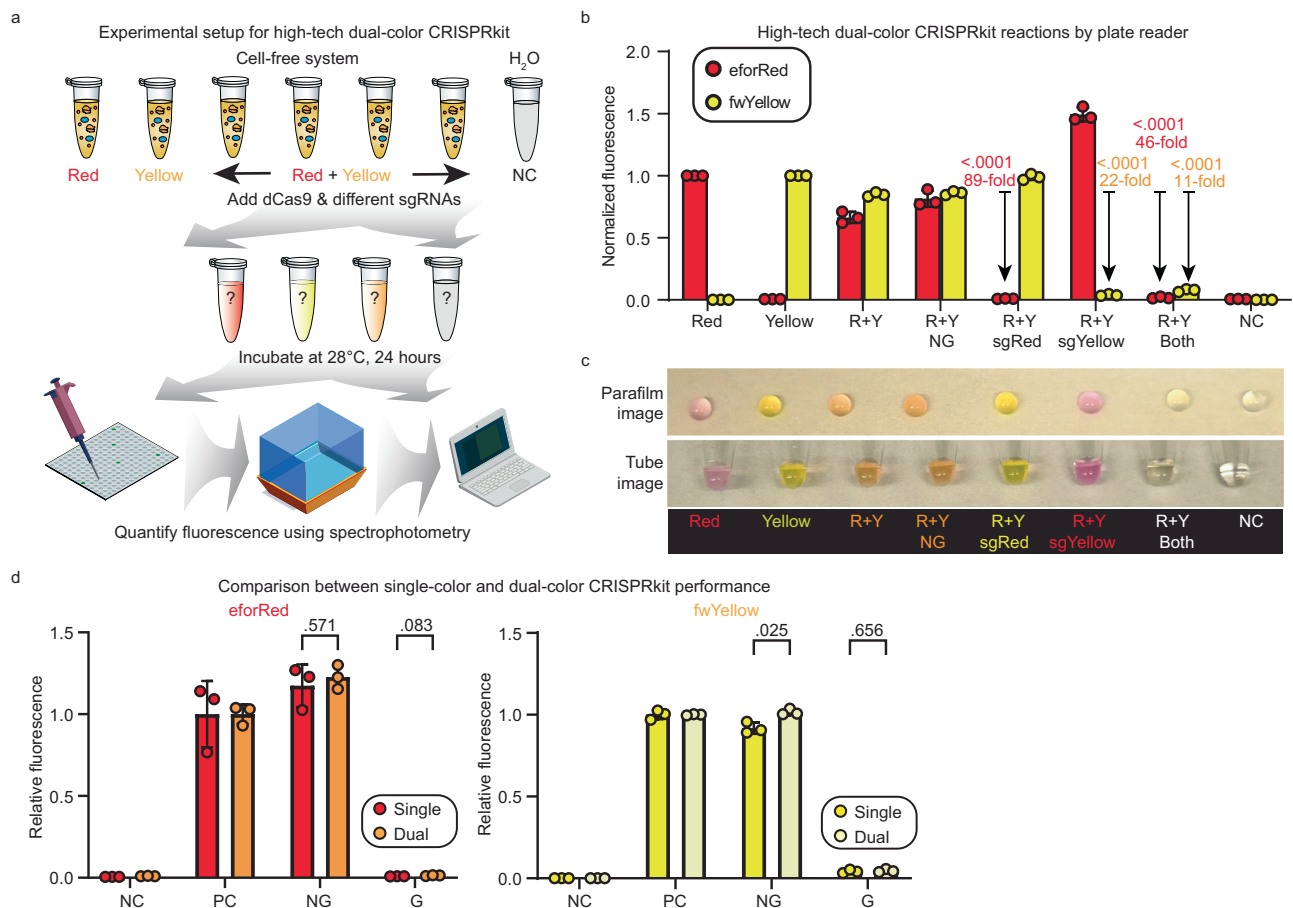


**Fig. 3 | Design and characterization of dual-color CRISPRkit using the high-tech setup.** **a** Experimental setup for high-tech dual-color CRISPRkit reactions. The CFS is mixed with one or two chromoprotein plasmids with one or two sgRNA plasmids, incubated at 28 °C for 24 h, and the fluorescence is quantified using a fluorescence plate reader. **b** Experimental data showing the performance of high-tech dual-color CRISPRkit reactions measured by a fluorescence plate reader. Each group of bars show eforRed or fwYellow single-color positive controls, eforRed +fwYellow dual-color positive control, with an empty sgRNA plasmid (NG), eforRed-targeting sgRNA (sgRed), fwYellow-targeting sgRNA (sgYellow), and both eforRed and fwYellow-targeting sgRNAs, and negative control (water only). **c** Smartphone images of the high-tech dual-color CRISPR kit reactions on a parafilm (top) or PCR tubes (bottom), after incubation at 28 °C for 24 h. Fold of repression is labeled for each group. **d** Comparison of chromoprotein expression between high-tech single-

color and dual-color CRISPRkit reactions. The graphs show the normalized fluorescence for eforRed (left) and fwYellow (right) in single-color or dual-color reactions to their positive controls (CFS + chromoprotein plasmid). For **b–d**, three biological replicates are plotted for each group, with biological replicate values being calculated from the mean of two technical replicates for the dual-color data. The bars represent the mean of biological replicates, and the error bars represent the standard deviation. For **b**, two one-way ANOVA were performed; p values generated by comparison of chosen conditions to no-guide control via Dunnett's multiple comparisons test are indicated above the chosen condition, above the fold of repression. For **d**, multiple two-tailed Student's t-test were performed with the Holm-Sidak correction; multiplicity-adjusted p values are indicated above each compared pair. Source data are provided as a Source Data file.

fluorescence plate reader (Fig. 3c). We note that equimolar expression of both eforRed and fwYellow generated an orange color in the reaction. Interestingly, the repression levels of chromoprotein were comparable in the dual-color and single-color experiments (Fig. 3d): for eforRed, we observed 89-fold of repression in a dual-color experiment compared to 126-fold of repression in the single-color experiment; for fwYellow, we observed the same 22-fold repression. The repression level was lower when using both sgRNAs in the dual-color expression (46-fold for eforRed and 11-fold for fwYellow). Nevertheless, this level of repression has generated distinct colors that can be easily discerned by the naked eye using smartphone images (Fig. 3c). Taken together, our experiment suggests that the dual-color CRISPRkit can be designed to generate visually distinct colors to offer facile readout.

### Designing and testing a frugal CRISPRkit by removing equipment requirements

Next, we designed a cost-effective and equipment-free CRISPRkit to increase accessibility. We eliminated the need for specialized lab equipment by substituting lab equipment with accessible alternatives (Fig. 4a). We reasoned that, instead of using pipettes and pipette tips, inoculation loops can be used to transfer liquid with volume around 1  $\mu$ L. To eliminate the incubator that provides accurate temperature and humidity control, we postulated that room temperature should be adequate to support sufficient cell-free protein production and CRISPRi activity. Furthermore, encouraged by our smartphone images taken for single-color and dual-color experiments, we hypothesized that a smartphone can be used in place of a fluorescence plate reader. Finally, to aid multi-color quantification using phone images, we developed an in-house algorithm termed CRISpectra and associated website (<http://ckitdual.com>) for user-friendly data analysis.

We first performed an experiment to verify whether room temperature (RT,  $-22^{\circ}\text{C}$ ) enabled efficient chromoprotein expression and CRISPRi activity using CFS (Fig. 4b). Using eforRed, we quantified the chromoprotein expression (without sgRNA) and repression (with sgRNA) using the fluorescence plate reader. Our data showed that the optimal temperature range to conduct the cell-free CRISPRi reaction is around  $28^{\circ}\text{C}$ . Notably, room temperature and  $37^{\circ}\text{C}$  showed strong expression and repression. On the contrary,  $4^{\circ}\text{C}$  and  $42^{\circ}\text{C}$  greatly diminished both protein production and CRISPRi activity. Therefore, we confirmed room temperature offers an acceptable condition for the CRISPRkit, thus eliminating the need for an incubator.

We next developed the CRISpectra algorithm to quantify color intensity, as a proxy for chromoprotein expression level (Methods). CRISpectra extracts the RGB (red-green-blue) values from individual pixels, averages the values of all pixels in a selected area in the image, and outputs normalized color intensity values for each reaction by comparing with the average RGB values of single-color reactions. Our results showed that using CRISpectra on smartphone images generated data for eforRed and fwYellow was consistent with those measured by a fluorescence plate reader (Supplementary Fig. 3a). Interestingly, our smartphone image method showed better fold of repression for aeBlue, which was more aligned with the visual observation. Comparing the CRISpectra analysis with plate reader data, we observed high correlation between samples for all three chromoproteins (Supplementary Fig. 3b). We further characterized the high-tech dual-color CRISPRkit experiments as shown in Fig. 3a using the CRISpectra algorithm and smartphone images (Supplementary Fig. 4a) and observed similarly highly correlation between CRISpectra analysis and plate reader data (Supplementary Fig. 4b). In summary, our data suggests that smartphone images and CRISpectra provide a reasonable approximation of chromoprotein expression as an alternative to the fluorescence or absorbance measurement by the plate reader.

We next performed a dual-color CRISPRi experiment in a 'low-tech' frugal setting, using inoculation loops to transfer liquids and incubating the reactions at room temperature for 24 h. Our data demonstrated strong and consistent CRISPRi repression of cognate chromoproteins in the presence of individual or double sgRNAs, measured by the fluorescence plate reader (Fig. 4c) or smartphone images characterized by CRISpectra (Fig. 4d). The reactions using the frugal setup showed visible and distinct colors (Fig. 4e). We also compared plate reader data with the CRISpectra algorithm and saw strong correlation between the two methods ( $R^2 = 0.907$  and  $0.943$  for eforRed and fwYellow, respectively, Fig. 4f). This experiment confirmed that the frugal CRISPR kit design and the CRISpectra method reliably reported CRISPRi activity without the need for equipment or proprietary software.

### CRISPRkit using in-house cell-free system to reduce the reagent costs

The above experiments have used commercially available CFS. To further reduce the cost of reagents, we manufactured in-house cell-free transcription-translation system (Methods). Using the same CRISPRkit experimental setting as shown in Fig. 2b, we characterized the production of eforRed, fwYellow, and aeBlue and repression by their cognate sgRNAs. We observed significant repression for each chromoprotein using in-house CFS, with eforRed, fwYellow, and aeBlue showing 47-fold, 5-fold, and 2.1-fold repression, respectively (Fig. 5a).

We next performed low-tech dual-color CRISPRkit experiments as shown in Fig. 4a using the in-house CFS with 10 biological replicates to verify whether the performance is consistent. Characterized by either fluorescence plate reader or smartphone image followed by CRISpectra analysis, we observed strong and significant repression of individual or both chromoproteins (Fig. 5b, c). This suggests that the in-house CFS provides a low-cost and reliable way to perform CRISPRkit experiments.

Furthermore, we estimated the cost of reagents per CRISPRkit using in-house CFS reagents to be \$1.13, and the cost of disposal plastic consumables per kit to be \$0.88 (Supplementary Table 4). This brings the total cost per CRISPRkit to \$2.01, making it significantly more affordable than previous educational CRISPR kits, which often cost over \$100 per kit<sup>10,12,13,25</sup>.

### Testing of the frugal CRISPR kits by high school students in a classroom setting

With an inexpensive and robust kit in hand, we next tested whether the frugal CRISPRkit can be used by high school students in a classroom setting (Fig. 6a). We streamlined the design of CRISPRkit to minimize its components and manufactured the frugal CRISPRkit in bulk (Fig. 6b). We also provided detailed manual, protocol, and learning contents (Supplementary Notes 1–5, Supplementary Fig. 5a, b).

A single high school student performed the CRISPRkit experiment 9 times over different days and got 8 experiments to work consistently using the CRISpectra algorithm (Fig. 6c), despite one experiment failing. Nevertheless, the colors from the samples in the working 8 experiments were visible and discernible (Supplementary Fig. 6a). We took the samples and quantified the performance of 8 experiments by the plate reader and observed consistent performance as those quantified by CRISpectra (Supplementary Fig. 6b). The performance of these experiments was also comparable but more variable than those performed in a laboratory setup (Fig. 4d). We attributed this higher variation to the accuracy of using inoculation loops in liquid transfer by the students.

We next distributed the CRISPRkit to a local high school class (Supplementary Notes 1–3). Approximately 40 students were organized into 17 groups, with most groups consisting of 2 students and a few having 3 students, each group performing one CRISPRkit

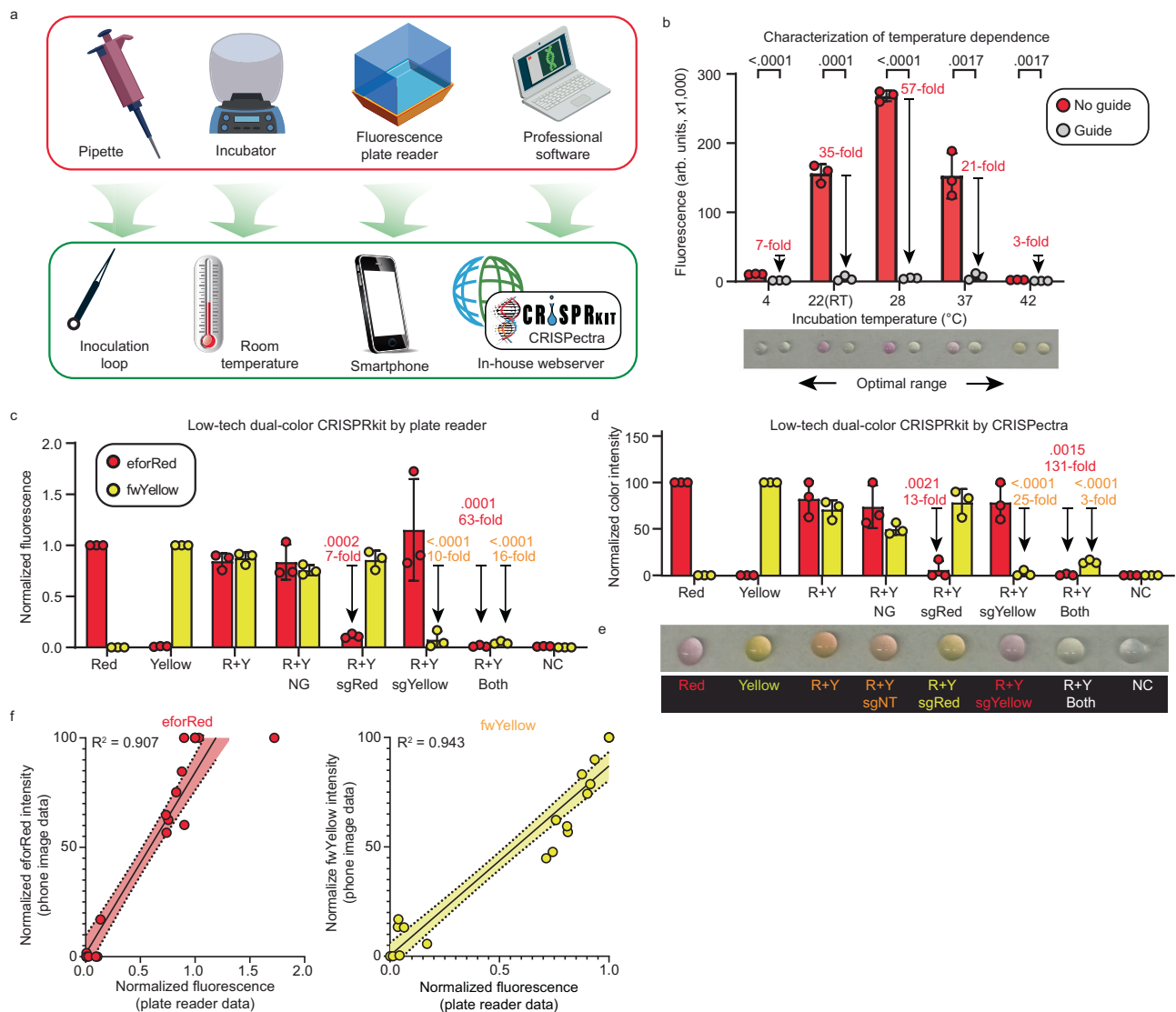


**Fig. 4 | Design and characterization of frugal low-tech dual-color CRISPRkit.**

**a** Schematic illustrating replacement of laboratory apparatus with frugal alternatives: pipettes with inoculation loops, incubator with room temperature setup, fluorescence plate reader with a smartphone, and professional analytical software with CRISPECTRA. **b** Performance characterization of the single-color CRISPRkit using eforRed at five different temperatures (4 °C to 42 °C). Reactions are incubated for 24 h. Red bars represent non-targeting sgRNA, and gray bars represent targeting sgRNA. A representative phone image of CRISPRkit reactions on parafilm is shown. Three biological replicates are plotted for each group, with mean fluorescence indicated by bars and standard deviation by error bars. Multiple two-tailed Student's *t*-tests with Holm-Sidak correction were performed; multiplicity-adjusted *p* values are indicated above each compared pair. **c** Experimental data showing low-tech dual-color CRISPRkit reactions measured by a fluorescence plate reader. From left to right, each group of bars (red – eforRed, yellow – fwYellow) show eforRed positive control, fwYellow positive control, eforRed + fwYellow dual-color positive control, dual-color with empty sgRNA plasmid (NG), dual-color with eforRed-targeting sgRNA (sgRed), dual-color with fwYellow-targeting sgRNA (sgYellow),

dual-color with both eforRed- and fwYellow-targeting sgRNAs, and negative control (water only). **d** Experimental data showing low-tech dual-color CRISPRkit reactions analyzed by CRISPECTRA. The order of the reactions mirrors **c**. For **c** and **d**, three biological replicates are plotted for each group, with biological replicate values being calculated from the mean of two technical replicates for **d**. The bars represent the mean of biological replicates, and the error bars represent the standard deviation. Two one-way ANOVA were performed; *p* values generated by comparison of chosen conditions to no-guide control via Dunnett's multiple comparisons test are indicated above the chosen condition, above the fold of repression. **e** A representative smartphone image of the CRISPRkit reactions on parafilm after 24 h at room temperature, following the same order as in **(d)**. **f** 2D scatter plots showing comparison of fluorescence plate reader data (x-axis) and phone image data (y-axis) for eforRed (left) and fwYellow (right). Individual dots represent biological replicates. Black lines represent the linear fit. Dotted lines represent 95% confidence interval.  $R^2$  values are shown for the linear regression. Source data are provided as a Source Data file.

experiment. On day 1, the teacher delivered a lecture on CRISPR and CRISPRi and demonstrated the procedure using one kit (demos followed the same outline as Supplementary Movies 1, 2). Following the demonstration, each group conducted the experiments according to the protocol. On day 2 (24 to 48 h is fine), the students used smartphones to take images and analyzed the data using CRISPECTRA. Except for 2 groups with failed positive controls, which made it difficult to analyze the fold of repression, 15 groups successfully generated the

desired outcomes with the CRISPRkit (Fig. 6d). The colors from the samples in all 17 groups' experiments were visible and discernible (Supplementary Fig. 7a). Additionally, we analyzed the samples using a plate reader and observed consistent performance with the results characterized by CRISPECTRA (Supplementary Fig. 7b).

We reasoned that teaching students the concept of efficiency and specificity helps improve their understanding of core concepts related to CRISPR experiments. Therefore, it is important to report the

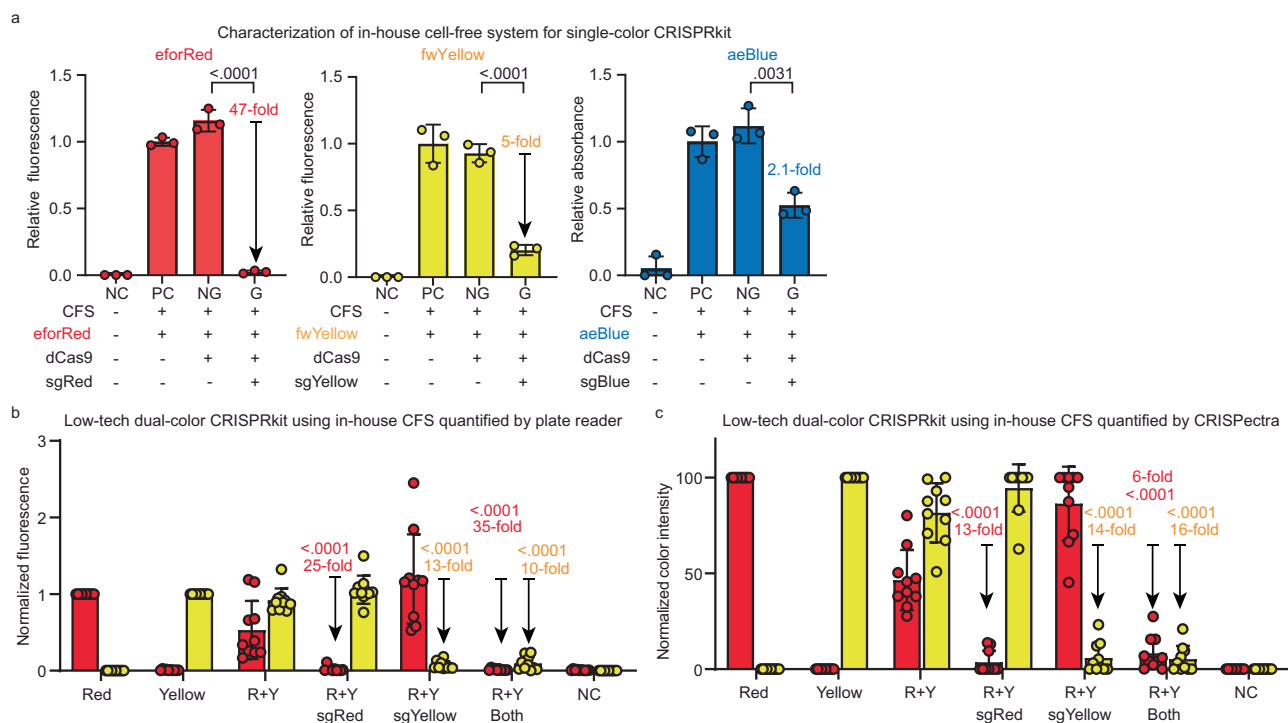


**Fig. 5 | Testing the frugal CRISPRkit using in-house cell-free system.**

**a** Experimental data showing the performance of single-color CRISPRkit reactions using in-house CFS. Three biological replicates calculated from mean of two technical replicates are plotted for each group. The bars represent the mean of biological replicates, and the error bars represent the standard deviation. Two-tailed Student's t-test was performed; p values are indicated above the no guide and guide condition bars. **b, c** Experimental data showing dual-color CRISPRkit reactions using in-house CFS, measured by a fluorescent plate reader (**b**) or smartphone images and analyzed by CRISPECTRA (**c**). From left to right, each group of bars (red – eforRed, yellow – fwYellow) show eforRed single-color positive control, fwYellow

single-color positive control, eforRed + fwYellow dual-color positive control, dual-color with eforRed-targeting sgRNA (sgRed), dual-color with fwYellow-targeting sgRNA (sgYellow), dual-color with both eforRed- and fwYellow-targeting sgRNAs, and negative control (water only). For **b, c**, ten biological replicates are plotted for each group. The bars represent the mean of biological replicates, and the error bars represent the standard deviation. Two one-way ANOVA were performed; p values generated by comparison of chosen conditions to no-guide control via Dunnett's multiple comparisons test are indicated above the chosen condition, above the fold of repression. Source data are provided as a Source Data file.

efficiency (the level of repression on the target gene) and specificity (the level of crosstalk repression on another gene) for CRISPR experiments. We calculated the efficiency and specificity of all experiments collected in the classroom consisting of 8 independent experiments by one student and 15 independent experiments by different groups (Supplementary Fig. 8). Our results showed high efficiency and specificity among most experiments performed by high school students (Fig. 6e).

### Expanding the frugal CRISPRkit as a versatile and modular educational module for genetic engineering in the high school classroom setting

We next expanded the utility of CRISPRkit towards hypothesis-driven experiments in the classroom. We reasoned that combining different chromoproteins provides different outcomes that can be directly observed without equipment, thus inspiring the students to formulate and execute their own plans using the frugal CRISPRkit.

We tested all possible combinations of eforRed, fwYellow, and aeBlue using CRISPRkit but without dCas9. Our results showed that combinations can generate a panel of visible colors (Fig. 7a). This forms a basis for using CRISPRkit to repress single or multiple chromoprotein genes and generate different visible outcomes, an opportunity for students to make their own designs in a 'guess-and-test' manner to figure out the composition of genes in a tube.

We next designed an experiment by mixing equimolar eforRed and aeBlue plasmids. In this module, the students would be unaware of which genes were in the tube but instructed to test their hypothesis using CRISPRkit (Fig. 7b, Supplementary Fig. 9). The students would be

instructed to work with the provided tube of genes and CRISPRkit with different sgRNAs to repress either fwyellow, eforRed, aeBlue, or their combinations to infer which genes are present. The standard CRISPRkit protocol (Supplementary Notes 2 & 3) will be provided to the student. As an example, the raw data from CRISPRkit reactions on the tube of mixture of eforRed and aeBlue is shown in Fig. 7c, which was qualitatively analyzed using the CRISPECTRA algorithm as shown in Fig. 7d. Based on this CRISPRkit result, the student can report the unknown genes in the tube as a mixture of red and blue genes.

We reasoned that there exists a panel of diverse chromoproteins that can be harnessed to build an expanded CRISPRkit, each with a specific targeting sgRNA, to enable more possibilities of such 'guess-and-test' experiments (Supplementary Fig. 10). Such experiments offer a cost-effective way for high school students to perform their designed CRISPR experiments, promoting their learning and inspiring their interests towards biotechnology. Beyond chromoprotein, we also tested and verified effective production and repression of a fluorescent protein, sfGFP, thus expanding its utility to other fluorescent proteins (Fig. 7e). To aid the effort for dissemination, we designed a user-friendly website (<https://crisprkit.org>) containing information of the CRISPR kit, protocols, and analysis algorithm, to help disseminate the kits among broad communities (Supplementary Fig. 11).

### Application of CRISPRkit to control melanin production and metabolic pathways

We next sought to expand CRISPRkit beyond chromoproteins and fluorescent proteins. Metabolism is a core concept in high school biology, but limited hands-on options are available for the students to



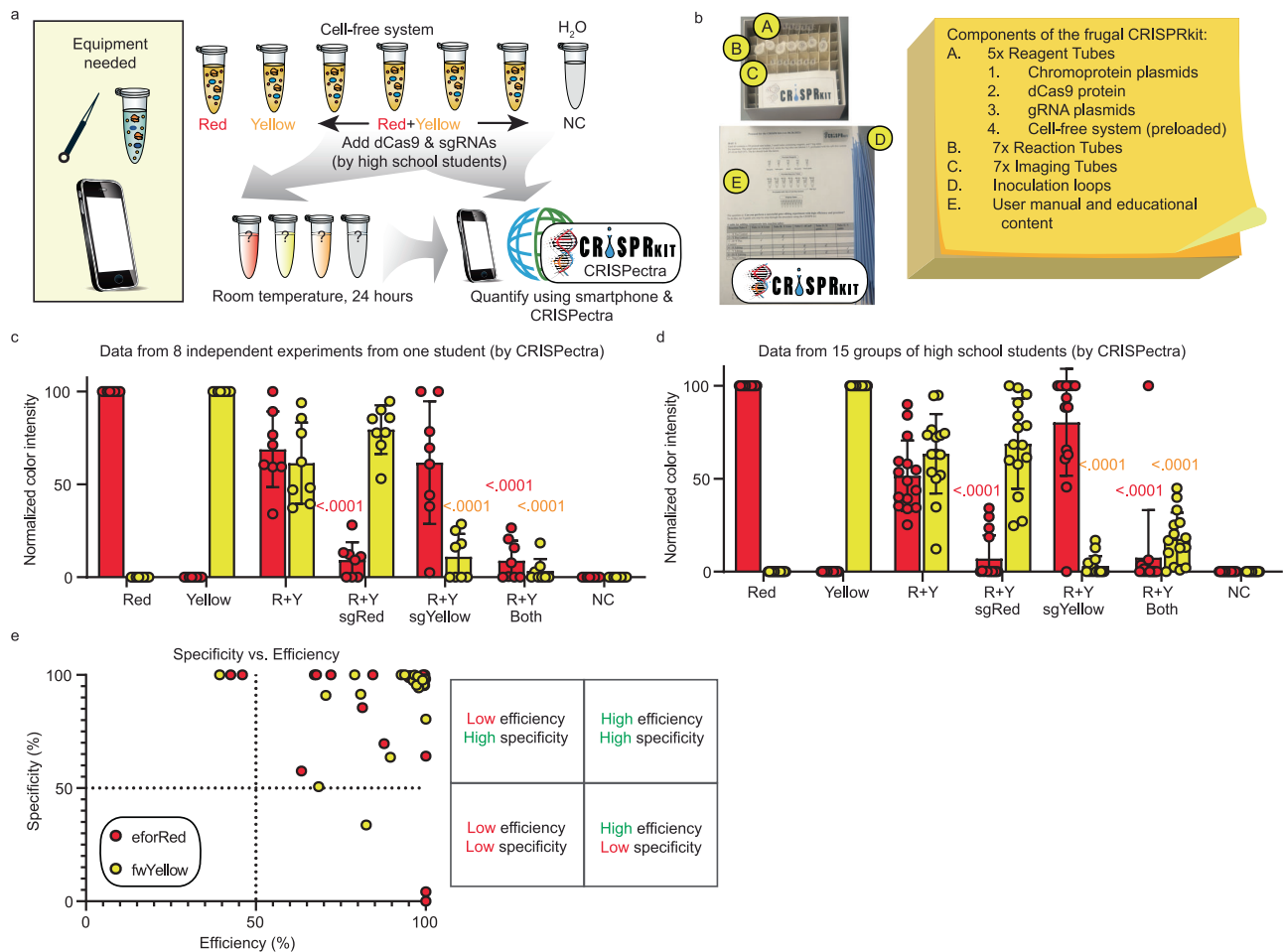


**Fig. 6 | Testing the frugal dual-color CRISPRkit by high school students in a classroom setting.** **a** Experimental setup of the frugal dual-color CRISPRkit in a frugal setting. The reagents are provided to the students, together with a detailed protocol. The students transfer the reagents including chromoprotein plasmids, dCas9, and sgRNA plasmids into reaction tubes preloaded with the cell-free system. The reactions are left at room temperature for 24 h. Smartphones are used to image the reactions and uploaded to CRISPRkit for image analysis. **b** Illustration of the components of the frugal CRISPRkit. A, Reagent tubes (5), containing the chromoprotein plasmid for eforRed, fwYellow, dCas9 protein, and sgRNA targeting eforRed or fwYellow. B, Reaction tubes (7, preloaded with the cell-free system). C, Imaging tubes (7), for the phone image purpose. D, Inoculation loops (17 loops for each kit, and 3 spare ones). E, User manual and protocol. **c** Experimental data from 8 independent CRISPRkit experiments performed by one high school student in the

frugal setting. **d** Experimental data from 15 independent CRISPRkit experiments performed by 15 groups of high school students in the classroom setting. For **c**, **d**, the bars represent the mean of biological replicates, and the error bars represent the standard deviation. Two one-way ANOVA were performed for each figure; p values generated by comparison of chosen conditions to no-guide control via Dunnett's multiple comparisons test are indicated above the chosen condition, above the fold of repression. **e** 2D scatter plot showing the calculated efficiency and specificity for each reaction for eforRed (red) and fwYellow (yellow). The top right quadrant shows reactions with high efficiency and high specificity. Individual dots represent biological replicates. Data points with both specificity and efficiency of 100% were jittered by <5% to facilitate visualization of many overlapping data points.

conduct experiments. Among potential metabolic pathways, melanin production has been an essential pathway in biology. Many organisms, including bacteria, fungi, plants, and animals (e.g., squid), possess metabolic pathways for melanin production for important biological purposes<sup>26–28</sup>. In human, melanin fulfills important functions including hair and skin pigmentation, photoprotection of the skin against UV light, and determination of differences in skin color among people<sup>29</sup>. Pigmentation of the skin results from the accumulation of melanin-containing melanosomes in the basal layer cells of the epidermis termed melanocytes. But such cellular systems are difficult to work with in a classroom setting. Therefore, it is important to develop CRISPRkit for regulating melanin production in a frugal setting.

Genetics plays a crucial role in determining the amount of melanin present in an individual's skin. Differences in skin pigmentation result from various forms of melanin, including eumelanin (black) and pheomelanin (red). Melanin synthesis begins with the hydroxylation of the amino acid tyrosine to L-3,4-dihydroxyphenylalanine (DOPA) in a

reaction catalyzed by an enzyme termed tyrosinase<sup>30</sup> (Fig. 8a). The conversion of DOPA to Dopakinone is also catalyzed by tyrosinase, which ultimately leads to melanin production via multiple steps (Fig. 8a). We hypothesized that controlling the production of the tyrosinase enzyme via CRISPRi should lead to production of different amount of melanin in the CFS and generate visible outcomes that are measurable by the frugal CRISPRkit.

To test this, we synthesized the tyrosinase gene (*melC*) derived from *Priestia megaterium* and cloned it onto our gene expression plasmid (Fig. 8b, c, Supplementary Fig. 12)<sup>31</sup>. We further designed 6 sgRNAs that target specific sequences along the *melC* protein-coding region, with 3 sgRNAs (#1–#3) targeting the template strand and 3 sgRNAs (#4–#6) targeting the non-template strand. We customized CRISPRkit to include a tyrosinase-producing plasmid (pmelC) and various sgRNA expression plasmids (sgmelC#1–#6) or a no-guide plasmid (NG) (Fig. 8c). Importantly, we supplemented the CFS with additional tyrosine (substrate) and Cu<sup>2+</sup>, which we have verified to be

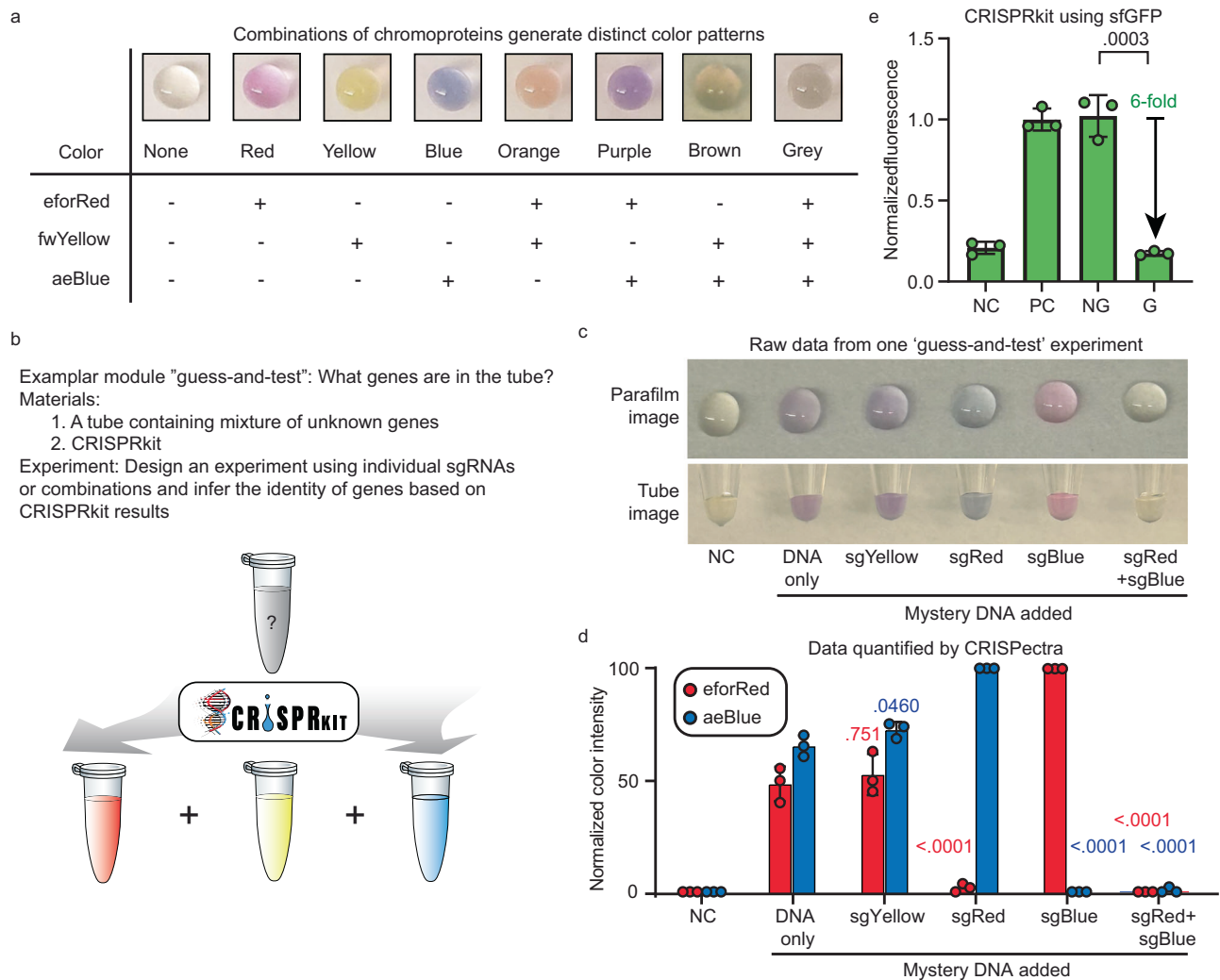


**Fig. 7 | An exemplar teaching module using the frugal CRISPRkit. a** Smartphone images of combinations of different chromoproteins in CFS reactions transferred to a parafilm. Conditions are listed below each droplet. **b** Schematic of a 'guess-and-test' experiment. The question asked is which genes are in the tube? A tube containing unknown plasmids encoding one or more chromoproteins and the frugal CRISPR kit are provided to the students. **c** The raw parafilm and tube images from one 'guess-and-test' experiment. **d** Experimental data from the 'guess-and-test' CRISPRkit experiment analyzed by CRISPECTRA. Three biological replicates calculated from mean of two technical replicates are plotted for each group. The bars represent the mean of biological replicates, and the error bars represent the

standard deviation. Two one-way ANOVA were performed; *p* values generated by comparison of chosen conditions to no-guide control via Dunnett's multiple comparisons test are indicated above the chosen condition, above the fold of repression. **e** Experimental data from using the frugal CRISPRkit experiment on sfGFP. Three biological replicates calculated from the mean of two technical replicates are plotted for each group. The bars represent the mean of biological replicates, and the error bars represent the standard deviation. Two-tailed Student's *t*-test was performed; *p* values are indicated above the no guide and guide condition bars. Source data are provided as a Source Data file.

essential for melanin production in the CFS. Different from the chromoprotein-based CRISPRkit, our experimental procedure is only 4 h as we have observed rapid melanin production due to a fast catalysis process.

We tested the performance of individual sgRNAs in repressing *melC* transcription, which should reduce production of melanin and pigmentation. As expected, both positive control (PC) and no-guide (NG) groups showed strong melanin production at 4 h, characterized by a plate reader or smartphone images and CRISPECTRA (Fig. 8d–f). In comparison, various sgRNAs showed significant reduction on melanin production, with the top 3 performing sgRNAs (#1, #5, #6) showing more than two orders of magnitude of reduction. The tube images showed distinct colors between dark and transparent. We also asked whether combining multiple sgRNAs can further enhance repression of *melC* and melanin production (Supplementary Fig. 13a). Interestingly, combining two functional sgRNAs showed improved repression (#1 & #3), while combining a functional sgRNA with a non-functional

sgRNA generally showed reduced repression (e.g., any group with #2) (Supplementary Fig. 13b–d). For students interested in exploring this melanin production and CRISPRi system themselves, we designed a CRISPRkit protocol and discussion questions (Supplementary Note 6). The application of CRISPRkit for controlling production of metabolites expands its utility, which can be used to educate students on complex biological concepts such as enzymes and metabolism (Supplementary Notes 1 and 7).

## Discussion

In this study, we designed and implemented an affordable CRISPRkit that can be broadly distributed to high school students to gain hands-on experiences on conducting CRISPR experiments. Compared to reported cell-free systems using CRISPR<sup>10,12,13,25</sup>, our CRISPRkit eliminates the need for equipment (e.g., pipettes, incubator, and imager), relies solely on smartphones for measurement, and utilizes an in-house CRISPECTRA algorithm for data analysis, which greatly increases

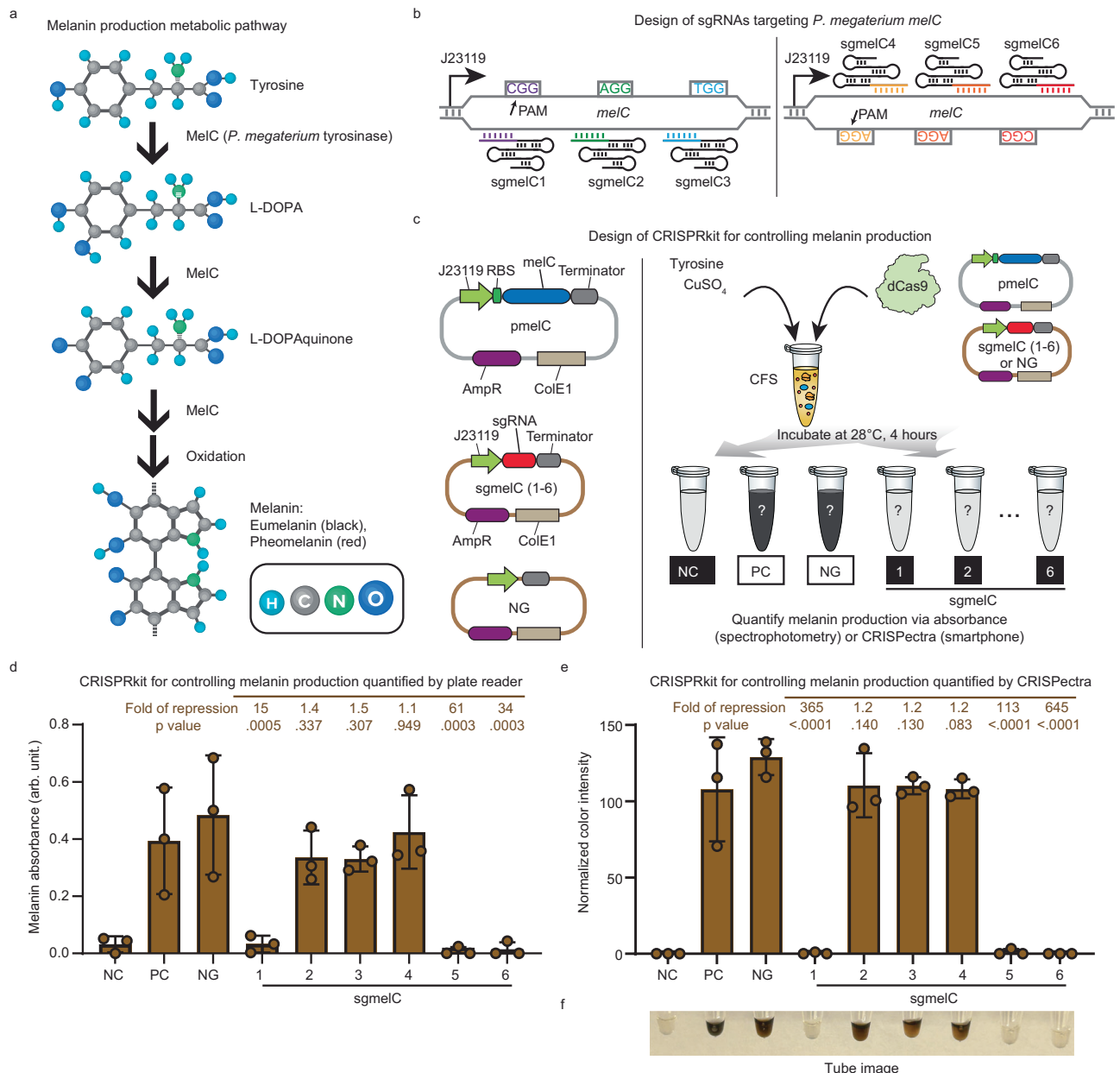


**Fig. 8 | CRISPRkit experiment for controlling melanin production.** **a** Schematic of the melanin production metabolic pathway. The *melC* tyrosinase converts tyrosine (substrate) to L-DOPA and L-Dopaquinone, which subsequently converts to melanin consisting of eumelanin or pheomelanin. **b** Design of sgRNAs that target the *melC* coding region on the template strand (left) or the non-template strand (right). The PAM for each sgRNA is shown. **c** Experimental setup for the high-tech single-color experiment using the CRISPRkit with different sgRNAs. After incubation at 28 °C for 4 h, we quantify the absorbance using a fluorescence plate reader or smartphone images and CRISPECTRA. **d, e** Experimental data showing CRISPRkit

reactions for controlling melanin production, measured by a fluorescent plate reader (**d**) or smartphone images and analyzed by CRISPECTRA (**e**). Three biological replicates are plotted for each group. The bars represent the mean of biological replicates, and the error bars represent the standard deviation. A one-way ANOVA was performed for each dataset; p values generated by comparison of chosen conditions to no-guide control via Dunnett's multiple comparisons test are indicated above the chosen condition, above the fold of repression. **f** Raw tube images showing one group of CRISPRkit reactions for controlling melanin production. Source data are provided as a Source Data file.

accessibility to students. By using in-house made CFS and plasmids, the estimated total cost of reagents and plastic consumables per CRISPRkit is \$2.01, which is significantly lower than the cost of previous educational CRISPR tools (Supplementary Table 4).

CRISPRkit eliminates the requirements for laboratory equipment and performs robustly in a classroom setting. We compared CRISPRkit designs using the cutting enzyme Cas9 for gene editing with the nuclease-dead dCas9 for gene regulation and opted for dCas9, which showed less leakage and better performance. Furthermore, the use of dCas9 can potentially reduce impact on the environment because dCas9 does not induce permanent DNA alterations. Our results

demonstrated that the frugal CRISPRkit without using pipettes or equipment performed comparably well to the CRISPR experiments using laboratory equipment. We developed an in-house data analysis algorithm, CRISPECTRA, to facilitate the quantification of chromoprotein expression and repression using smartphone images. Classroom teaching using CRISPRkit confirmed the robustness of its performance when used by high school students who had no prior experience in CRISPR experiments. Finally, we demonstrated that CRISPRkit provides a broad platform in synthetic biology, which can be expanded to more complex biological concepts such as metabolic pathways (e.g., melanin production). These experiments together suggest that

CRISPRkit offers a powerful, versatile, and robust tool to offer hands-on experiences to high school students.

We demonstrated that CRISPRkit offers an expandable platform for users to add their own content. Besides chromoproteins, we showed that CRISPRkit can work robustly with fluorescent proteins and metabolic pathways such as melanin production. For example, by designing sgRNAs that specifically repress transcription of *melC* tyrosinase, we can use CRISPRkit to modulate enzyme expression and characterize melanin production using CRISPR Spectra. We expect the frugal CRISPRkit could be further expanded to include additional biotechnology content in the future, such as production of biomaterials and sequestration of CO<sub>2</sub>.

We tested CRISPRkit in a classroom setting. The CRISPRkit protocol is simple to follow, taking 30 min to perform and offering a flexible module that can be added to curricula. Among the 17 groups of students, 15 groups were able to get CRISPRkit to work (Fig. 6c–e). From our analysis of successful and failed frugal CRISPRkit reactions, the performance of CRISPRkit is mainly dependent on the quality of purified plasmid DNA and the accuracy of liquid transfer. For example, we noticed drastically different performance of chromoprotein production using suboptimally purified chromoprotein plasmids. The failed classroom test groups (2 out of 17) using CRISPRkit were due to failures in transferring liquid properly. For taking smartphone images, lighting and shading can affect data quality. We suggest ample lighting and avoiding shading when taking images. In CRISPR Spectra, we have designed the algorithm to minimize the lighting impacts.

To facilitate adoption of CRISPRkit, we designed a wide range of online resources that includes protocols, instructional videos, a CRISPR Spectra portal, and a reagent request form. Supplementary Table 5 summarizes the permanent URLs to these resources. We provide a core concept summary in Supplementary Note 1, a detailed dual-color CRISPRkit protocol in Supplementary Notes 2 (protocol - day 1) and 3 (protocol - day 2), a worksheet document for students in Supplementary Note 4, detailed instructions for teachers to set up experiments in Supplementary Note 5, a detailed melanin CRISPRkit protocol and worksheet in Supplementary Note 6, and exemplar CRISPRkit teaching slides in Supplementary Note 7.

Providing equitable and accessible K-12 education on innovative biotechnologies requires safe and cost-effective tools, which are currently limited. CRISPR technology has broad impact and has become a core concept in modern biotechnology. We envision that the CRISPRkit can be manufactured in large quantities and distributed to many high school classrooms to facilitate courses such as AP Biology. With the low-cost design, we believe the frugal CRISPRkit can eliminate financial barriers and allow teachers to adopt for their teaching and learning purposes. A freezer was all needed for the long-term storage of reagents at -20 °C. We anticipate that the components can be further freeze dried to enable room-temperature storage<sup>25,32</sup>.

In the future, we will expand CRISPRkit to more proteins with diverse colors and enzymes with tangible readouts. For each gene, we will characterize specific sgRNAs to ensure efficient CRISPRi reactions. It is also possible to incorporate the CRISPR activation (CRISPRa) system with the orthogonal CRISPRi to enable multiplexed up- and down-regulation of different genes in a genetic circuit. CRISPRkit offers a valuable education tool for students and the public to learn about the revolutionary CRISPR technology, contributing to equitable and accessible education for all socioeconomic backgrounds.

## Methods

### Ethics statement

This research complies with all relevant ethical regulations. The study adhered to ethical standards to ensure the protection and confidentiality of all participants. It involved high school teachers, who guided high school students in using the CRISPRkit as part of their

biology curriculum. Participation in the study was voluntary and anonymous, with no personally identifiable information collected at any stage. Informed consent was obtained from the teachers and all participants were informed about the nature and purpose of the study. The collected data was securely stored and analyzed to assess the effectiveness of the kits. Consent was obtained for publishing the experimental data in this manuscript. The study was conducted with careful consideration of researcher contributions and authorship criteria to promote greater equity in our research collaborations. This research was reviewed by the Stanford University Institutional Review Board (IRB) and determined not to be human research.

### Plasmid cloning and preparation

All primers were designed in Benchling and synthesized by Stanford's Protein and Nucleic Acid Facility. Primer sequences can be viewed in Supplementary Table 6. Gibson assembly was used for the construction of pSLQ3533 (eforRed plasmid) and pSLQ3534 (fwYellow plasmid). To clone the chromoprotein plasmids, pSLQ220 was digested by NheI and XhoI. gBlocks encoding the fwYellow and eforRed genes were ordered from IDT. gBlocks and the digested vector were joined using an NEBuilder HiFi DNA Assembly kit during a 1-hour (hr) incubation at 50 °C. Plasmid DNA from the Gibson assembly reaction was then transformed into Stellar Competent Cells (Takara Bio).

In-Fusion cloning (Takara Bio) was used for the construction of plasmid pSLQ14101 (aeBlue plasmid). pSLQ3533 was digested by restriction enzymes BglII and XhoI. Plasmid encoding the aeBlue gene was ordered from Addgene (#117846). The aeBlue chromoprotein gene was amplified in a PCR reaction using a KAPA Hi-Fi kit (Roche). Following electrophoresis, PCR products were extracted from a gel using a NucleoSpin Gel and PCR Cleanup kit (Machery-Nagel). Purified PCR products were inserted into the digested backbone using an In-Fusion reaction. Plasmid DNA from the In-Fusion reaction was then transformed into Stellar Competent Cells (Takara Bio).

In-Fusion cloning (Takara Bio) was used for the construction of plasmid pSLQ13960 (*melC* tyrosinase expression plasmid). The backbone plasmid pSLQ3533 was digested by restriction enzymes EcoRI and XhoI. The *melC* gene (GenBank: QIZ65822.1) was synthesized (Twist Bioscience) and amplified in a PCR reaction using a KAPA Hi-Fi kit (Roche). Following electrophoresis, PCR products were extracted from a gel using a NucleoSpin Gel and PCR Cleanup kit (Machery-Nagel). Purified PCR products were inserted into the digested backbone using an In-Fusion reaction. Plasmid DNA from the In-Fusion reaction was transformed into Stellar Competent Cells (Takara Bio).

To design sgRNAs, we selected a 20-bp sequence with a nearby PAM sequence (NGG) on the coding region of each chromoprotein as the target site and used algorithm CRISPR-ERA to verify their specificity<sup>24</sup>. For the cloning of pSLQ3538 (eforRed-targeting sgRNA plasmid), pSLQ14107 (fwYellow-targeting sgRNA plasmid), pSLQ14103 (aeBlue-targeting sgRNA plasmid), pSLQ14108 (sgmelC1), pSLQ14109 (sgmelC2), pSLQ14110 (sgmelC3), pSLQ14111 (sgmelC4), pSLQ14112 (sgmelC5), and pSLQ14113 (sgmelC6), forward and reverse primers for a full-plasmid PCR were designed. sgsgGFP was obtained directly from a previously published work<sup>17</sup>. Forward and reverse primers contained 15 base pair regions homologous to each other for joining in an In-Fusion reaction. The forward primers contained a region encoding the desired spacer sequence for the sgRNA. pSLQ3529 was used as the DNA template for a full-plasmid PCR using the described primers, which was performed using a KAPA Hi-Fi kit. Following electrophoresis, PCR products were extracted from a gel using a NucleoSpin Gel and PCR Cleanup kit. Purified PCR products were circularized using an In-Fusion reaction. Plasmid DNA from the In-Fusion reaction was then transformed into Stellar Competent Cells.

pSLQ3533, pSLQ3534, pSLQ3538, pSLQ13960, pSLQ14103, pSLQ14101, pSLQ14107, pSLQ14108, pSLQ14109, pSLQ14110, pSLQ14111, pSLQ14112, and pSLQ14113 constructs were selected on LB-



agar supplemented with 100  $\mu\text{g mL}^{-1}$  carbenicillin. Sequence-verified clones were purified using a Plasmid Plus Midi Kit (Qiagen), then purified again using a Nucleospin Gel and PCR Clean-Up Mini kit (Machery-Nagel). The final purification step is essential to ensure optimal performance of plasmids in both myTXTL Sigma 70 Master Mix and our in-house CFS.

### High-tech CRISPRkit reaction using myTXTL

All fluid transfer was performed using micropipettes. MyTXTL Sigma 70 Master Mix was purchased from Daicel Arbor Biosciences and vortexed and spun down in a centrifuge before each experiment. 9  $\mu\text{L}$  of myTXTL Sigma 70 Master Mix was allotted into 1.5 mL Eppendorf tubes. All other reaction components, if included in a reaction, were added to the following target concentrations: 2.1  $\text{ng } \mu\text{L}^{-1}$  dCas9 V3 protein (IDT, cat no. 1081066); 5 nM chromoprotein plasmid DNA; 2.5 nM sgRNA plasmid DNA. Water was added to bring the final reaction volume to 15  $\mu\text{L}$ . Reactions were incubated at 28 °C for 24 h.

### Low-tech CRISPRkit reaction using myTXTL

A total of 10  $\mu\text{L}$  of myTXTL Sigma 70 Master Mix was allotted into 1.5 mL Eppendorf tubes. All other reaction components, if included in a given reaction, were added to the following target concentrations: 2.1  $\text{ng}/\mu\text{L}$  dCas9 V3 protein (IDT); 5 nM chromoprotein plasmid DNA; 2.5 nM sgRNA plasmid DNA. Reagent stocks were diluted such that adding 1  $\mu\text{L}$  of each to a given reaction would achieve the target concentration. For the addition of each reaction component, a 1  $\mu\text{L}$  inoculation loop was first inserted into the stock solution and twirled several times while fully submerged. Then the loop was removed and checked by eye to ensure fluid was present within the loop. The loop was then inserted into the reaction mixture and twirled several times while fully submerged. Loops were then rinsed with running water and dried with a paper towel for later reuse. Enough water to bring the final reaction volume to 15  $\mu\text{L}$  was pipetted into each reaction. Reactions were incubated at room temperature for 24 h.

### Fluorescence and absorbance quantification using the plate reader

A standardized volume (5  $\mu\text{L}$  for tests using myTXTL Sigma 70 Master Mix, 2.5  $\mu\text{L}$  for tests using chromoproteins or fluorescent proteins in our in-house CFS, or 5  $\mu\text{L}$  for tests producing tyrosinase and melanin in our in-house CFS) of each sample was pipetted into a Hard-Shell 384-well clear microplate (Bio-Rad #HSP3805), and fluorescence and absorbance readings were taken by a Synergy H1 microplate reader (BioTek) using BioTek Gen5 version 3.02. The excitation and emission wavelengths used to quantify fluorescence of eforRed, fwYellow, and sfGFP were as follows: eforRed ex 589 nm, em 615 nm; fwYellow ex 520 nm, em 550 nm; sfGFP ex 488 nm, em 510 nm. The absorbance wavelengths used to quantify the absorbance of aeBlue and melanin were 593 nm and 670 nm, respectively.

### In-house CFS preparation

**Cell extract preparation.** Cell extract was prepared for expression from endogenous transcriptional machinery<sup>33</sup>. First, 2xYTP (16 g/L tryptone, 10 g/L yeast extract, 5 g/L sodium chloride, 7 g/L potassium phosphate dibasic, and 3 g/L potassium phosphate monobasic adjusted to pH 7.2) was inoculated with saturated overnight culture of BL21 Star (DE3) at an optical density (OD<sub>600</sub>) of 0.06. The culture was incubated at 37 °C at 220 RPM. Between OD<sub>600</sub> of 0.4–0.6, IPTG to a final concentration of 0.5 mM was added to the culture to induce T7 RNA polymerase expression. At OD<sub>600</sub> = 3.0, cells were harvested by centrifugation at 5000xg for 15 min at 4 °C. The cell pellets were washed three times in 25 mL wash buffer (50 mM Tris, 14 mM Mg-glutamate, 60 mM K-glutamate, 2 mM DTT, brought to pH 7.7 with acetic acid). The first two centrifugations between washes were at

5000 x g for 10 min at 4 °C. The final centrifugation was at 7000 x g for 10 min at 4 °C. Then, the pellets were resuspended in 1 mL wash buffer/g pellet. For lysis, cells were homogenized by being passed once through an Avestin EmulsiFlex-B15 at 20,000 to 25,000 psig. Immediately after homogenization, the lysed cell solution was aliquoted into 1.7 mL Eppendorf tubes and dithiothreitol (DTT) was added to each tube to a final concentration of 3 mM. The tubes were then centrifuged at 12,000 x g for 10 min at 4 °C. For ribosomal runoff reaction, the supernatant was collected into a new tube and incubated at 37 °C at 220 rpm for 80 min. Next, the extract was centrifuged at 12,000 x g for 10 min at 4 °C. For dialysis, the supernatant was collected into a 10 kDa molecular-weight cut-off membrane and dialyzed against dialysis buffer (14 mM Mg-glutamate, 60 mM K-glutamate, 5 mM Tris, 1 mM DTT, pH 7.7) for 3 h without exchange. Then, the extract was collected from the dialysis cassettes into new Eppendorf tubes and centrifuged at 12,000 x g for 10 min at 4 °C. After this final centrifugation, the supernatant was collected, aliquoted and flash-frozen in liquid nitrogen. Extract is stored at –80 °C.

**In-house CFS pre-mix preparation.** A pre-mix solution was prepared on ice using pipettes. The final individual CFS reactions had a total volume of 15  $\mu\text{L}$ , and the following components were added to the pre-mix such that adding 8.8  $\mu\text{L}$  of the pre-mix to each reaction would reach the given target concentrations: 12 mM magnesium glutamate, 10 mM ammonium glutamate, 130 mM potassium glutamate, 1.2 mM ATP, 85 mM GTP, 85 mM UTP, 85 mM CTP, 0.34 mg/mL folinic acid, 17 mg/mL yeast tRNA, 4 mM NAD, 27 mM CoA, 4 mM oxalic acid, 1 mM putrescine, 1.5 mM spermidine, 57 mM HEPES, 2 mM amino acids, 0.3 M PEP. Finally, cell extract was added to 30% final reaction volume.

### CRISPRkit chromoprotein/fluorescent protein reaction using in-house CFS

A total of 8.8  $\mu\text{L}$  of the pre-mix solution was allotted into 1.5 mL Eppendorf tubes using pipettes. All other reaction components, if included in a given reaction, were added to the following target concentrations: 2.1  $\text{ng}/\mu\text{L}$  dCas9 V3 protein (IDT); 10 nM chromoprotein plasmid DNA; 5 nM sgRNA plasmid DNA. Reagent stocks were diluted such that adding 1  $\mu\text{L}$  of each to a given reaction would achieve the target concentration. For low-tech experiments, inoculation loops were used for fluid transfer. For high-tech experiments, pipettes were used for fluid transfer. Enough water to bring the final reaction volume to 15  $\mu\text{L}$  was pipetted into each reaction. High-tech reactions were incubated at 28 °C. Low-tech reactions were incubated at room temperature.

### CRISPRkit melanin production reaction using in-house CFS

A total of 8.8  $\mu\text{L}$  of the pre-mix solution was allotted into 1.5 mL Eppendorf tubes using pipettes.  $\text{CuSO}_4 \cdot 5\text{H}_2\text{O}$  and L-tyrosine were added to final concentrations of 50  $\mu\text{g}/\text{mL}$  and 800  $\mu\text{g}/\text{mL}$ , respectively to all reactions<sup>34,35</sup>. All other reaction components, if included in a given reaction, were added to the following target concentrations: 2.1  $\text{ng}/\mu\text{L}$  dCas9 V3 protein (IDT); 10 nM pSLQ13960; 5 nM sgRNA plasmid DNA. Pipettes were used for all fluid transfer. Reactions were then incubated for 4 h at 28 °C.

### Image acquisition and pre-processing for smartphone-based data analysis

**Sample preparation.** For image acquisition, 4  $\mu\text{L}$  aliquots from each reaction tube were sequentially transferred onto parafilm.

**Image acquisition.** All experimental images were captured using an iPhone 14. Each image was taken in the same laboratory space equipped with consistent and optimal lighting conditions. The imaging angle was maintained at a slightly slanted angle relative to the

parafilm's surface at approximately an arm's length. This enabled the concealment of shadows to mitigate glare.

**Image segmentation and pre-processing.** After image acquisition, the images were manually cropped in a rectangular shape within the circular regions of the liquid droplets on the parafilm. Once segmented, the images were either retained in their original state or subjected to a minimum filter using the FIJI (ImageJ) software platform if image glare is deemed too significant. The minimum filter operates through grayscale erosion, replacing each pixel in an image with the smallest pixel value in its proximate neighborhood. This step is particularly vital in instances where an image manifests pronounced glare, as the filter effectively attenuates prominent bright spots. For images necessitating this filter, a radius equivalent to half of the image's pixel width was selected.

**Expression analysis.** Following the pre-processing stage, all the images were then fed into the phone-data analysis algorithm CRISPEctra for color intensity expression analysis.

### CRISPEctra – a smartphone-based data analysis pipeline for crisprkit experiments

**RGB-value extraction.** Each image represents a distinct experimental condition. The primary RGB (Red, Green, Blue) values were extracted from these images, and their mean values  $u_r, u_g, u_b$  computed using:

$$\mu_{R,G,B} = \frac{1}{N} \sum_{i=1}^N (R, G, B)_i \quad (1)$$

where N is the total number of pixels in the image.

### Negative control normalization

There were two foundational controls in each experiment: the Negative Control (NC) and the Positive Control (PC). The NC was established using only water, serving as a baseline, while the PC incorporated solely the chromoprotein gene, functioning as a benchmark for maximum intensity. Beyond these controls, the experimental conditions included targeting sgRNA (G) and no sgRNA (NG), capturing the varying dynamics of CRISPR interactions.

To account for non-specific signals and background noise, RGB values across all conditions were normalized against those obtained from the Negative Control (NC) condition. Specifically, for each condition  $i$  and its respective channel  $j$  (R, G, B), the values were adjusted using:

Let:

- $i$  be the index for the condition (e.g., NC, PC, condition 3, 4 ...)
- $j$  represent the channel (R, G, B) With this, the adjusted value for a specific channel in a specific condition can be given as:

$$\text{Adjusted Value}_{i,j} = \text{Original Value}_{i,j} - \text{NC Value}_j \quad (2)$$

Where:

- $\text{Original Value}_{i,j}$  is the value for the  $j^{\text{th}}$  channel (R, G, B) for the  $i^{\text{th}}$  condition.
- $\text{NC Value}_j$  is the value for the  $j^{\text{th}}$  channel in the NC condition.

**Dimensional reduction.** Next, we employed dimensional reduction on the RGB values of each experimental condition. This transformed the 3-dimensional RGB data of each condition into a singular representative value, thus condensing the color information into a quantifiable metric.

Our paper primarily presents two types of experiments. The first involves a singular chromoprotein, focusing on measuring the exclusive expression of this protein. The second delves into dual color

experiments, which included reactions with two distinct chromoproteins. This necessitated the extraction of intensity levels for both colors. We will now explain how the computation applied to both types of experiments.

**For single color.** When the experiment involved only one chromoprotein of color A, the reference vector,  $Vector_A$ , was derived from the RGB values of the PC condition, which corresponded to the condition where only color A was present in the cell-free mix. Mathematically, the magnitude of this vector is given by:

$$||Vector_A|| = \sqrt{Vector_{A,R}^2 + Vector_{A,G}^2 + Vector_{A,B}^2} \quad (3)$$

Where:

- $Vector_{A,R}, Vector_{A,G}, Vector_{A,B}$  represents the components of the PC  $Vector_A$  in the red, green, and blue channels, respectively. For instance, within the context of the paper's single-color experiments, consider an experiment with four conditions: NC, PC, NG, and G. After the initial step of normalizing each of the RGB values with the NC values, each condition still retained three RGB values. The dimensional reduction step was thus implemented to transform the three-dimensional data into one singular, representative value for each condition. The mathematical representation of the projection is as follows: For each condition  $i$ :

$$\text{Projection}_{A,i} = \frac{\text{Condition}_i \cdot Vector_A}{||Vector_A||} \quad (4)$$

Where:

- $\text{Projection}_{A,i}$  represents the singular value describing the intensity level of color A in condition  $i$ .
- Condition  $i$  represents the RGB values of the  $i^{\text{th}}$  condition, which are then subjected to a dot product operation with the RGB values of the positive control  $Vector_A$ .

Since there were 4 conditions, 4 projections were made to transform the dataset from its original 12 values—attributed to 3 RGB components across 4 conditions—to just 4 distinct values. Each of these values corresponded uniquely to one of the conditions: NC, PC, NG, and G, providing a representation of the intensity level of the color A chromoprotein in each respective condition.

**For dual color.** When the experiment involved two chromoproteins of color A and color B, we independently extracted the intensity levels for each chromoprotein. A two-step projection methodology is implemented, where each color was computed separately.

Same as the single-color experiments, for the first chromoprotein color A, the reference vector,  $Vector_A$ , was derived from the RGB values of the PC condition for color A.

We also computed the second reference vector,  $Vector_B$ , derived from the RGB values of the PC condition for the second chromoprotein - color B. The two projections are mathematically defined as:

For each condition  $i$ :

$$\text{Projection}_{A,i} = \frac{\text{Condition}_i \cdot Vector_A}{||Vector_A||} \quad (4)$$

And

$$\text{Projection}_{B,i} = \frac{\text{Condition}_i \cdot Vector_B}{||Vector_B||} \quad (5)$$

This allowed for the extraction of two unique intensity values for each condition from its original RGB values, one for each of the two

chromoproteins. For instance, within the context of the paper's dual-color experiments, consider an experiment with 7 conditions: *NC*, *PC* (color A only), *PC* (color B only), *PC* (color A + color B), *G<sub>A</sub>* (targeting color A), *G* (targeting color B), and *G<sub>A+B</sub>* (targeting both color A + color B). The projections generated a total of 14 unique values: a set of 7 for each condition for color A, and 7 for each condition for color B.

**Crosstalk minimization.** In dual-color experiments, color overlap between different chromoproteins could lead to inaccurate intensity readings. To correct this, we calculated the shifts for each color and adjusted their projected values accordingly.

In the context of single-color experiments, where only one chromoprotein is present, this adjustment step was not necessary.

**Calculation of shifts:** Color A shift per Color B value:

$$\text{Shift}_A = \frac{\text{Projected Value}_{A2}}{\text{Projected Value}_{B2}} \quad (6)$$

*Projected Value<sub>A2</sub>* denotes the projection value of *PC* (color B only) for color A, while *Projected Value<sub>B2</sub>* denotes the projection value of *PC* (color B only) of color B.

Color B shift per Color A value:

$$\text{Shift}_B = \frac{\text{Projected Value}_{B1}}{\text{Projected Value}_{A1}} \quad (7)$$

*Projected Value<sub>A1</sub>* denotes the projection value of *PC* (color A only) for color A, while *Projected Value<sub>B2</sub>* denotes the projection value of *PC* (color A only) of color B.

**Adjustment of projected values.** Using these shift values, we then calculated adjusted values for color A and color B, mathematically defined as:

For each color A condition *i*:

$$\text{Adjusted Value}_{A,i} = \text{Original Value}_{A,i} - \text{Shift}_A \cdot \text{Value}_{B,i} \quad (8)$$

For each color B condition *i*:

$$\text{Adjusted Value}_{A,i} = \text{Original Value}_{B,i} - \text{Shift}_B \cdot \text{Value}_{A,i} \quad (9)$$

These adjustments subtracted the influence of one color from the other, ensuring that the resulting values purely represented each chromoprotein's intensity level. This calibration ensures that when assessing the intensity of a specific chromoprotein, the projection value attributed to the contrasting color was nullified. For instance, when evaluating Color A's projection intensity values for the Color B *PC* (color B only) condition, its entry is 0, and vice versa.

In the final step, for both single and dual color experiments, all derived values were normalized to the respective color's *PC* value. This normalization effectively expressed each condition as a percentage relative to the *PC*'s intensity level. As a result, the *PC* assumed a value of 1, with all other condition values being presented as ratios in relation to this benchmark.

**Graphical representation and adjustments.** Upon obtaining the normalized values, additional adjustments were made to enhance the clarity and interpretability of the plots:

**Scaling for clarity.** All values were multiplied by 100. This scaling ensured that the *NC* condition had a value of 0, with the *PC* peaking at 100, offering a more intuitive percentage-based interpretation of the results.

**Negative value treatment.** To better reflect biological reality, any values that became negative after adjustments were reset to 0. This

adjustment ensured that the graphical depiction was consistent with the understanding that a negative value is biologically implausible for gene expression.

**Plotting.** The graphs were then plotted on Prism 9 (GraphPad) using these adjusted values for all phone imagery data.

### Correlation of smartphone-based data and plate reader data

To assess the efficacy of the phone-based method of measuring color intensity in approximating gene expression levels, its results were benchmarked against data obtained from a high-tech plate reader through correlation analysis.

**Data plotting.** The collected data sets were plotted on a scatter plot using DataGraph (Visual Data Tools). Each point on this plot represents an experimental condition, with its X-coordinate denoting the plate reader value and its Y-coordinate indicating the phone-based value.

**Regression and correlation analysis.** A linear regression analysis was performed on the plotted data to generate the line of best fit. The strength and direction of the linear relationship between the two datasets were quantified using the *R*<sup>2</sup> (Pearson correlation coefficient) value. A value close to 1 indicates a strong positive correlation between the phone-based and plate reader data, suggesting the phone-based method's robustness. The confidence interval is also shown, providing a range within which the true regression line is likely to fall, indicating the precision of the regression estimate.

### Analysis of CRISPRi gene repression efficiency and specificity

To assess the performance of the CRISPRi system in terms of its gene repression capability for dual color experiments, two key metrics were plotted: Efficiency and Specificity.

**Efficiency.** The efficiency metric reflects the ability of the CRISPRi system to selectively target and repress gene expression. It is calculated based on the reduction in the expression of the targeted gene compared to a condition where both genes (Red and Yellow) are expressed.

#### For yellow targeting in single

$$\text{Efficiency}_{\text{Yellow}_s} = 1 - \frac{\text{Yellow Targeting}(\text{yellow value})}{\text{Red} + \text{Yellow}(\text{yellow value})} \quad (10)$$

#### For yellow targeting in both

$$\text{Efficiency}_{\text{Yellow}_b} = 1 - \frac{\text{Both Targeting}(\text{yellow value})}{\text{Red} + \text{Yellow}(\text{yellow value})} \quad (11)$$

#### For red targeting in single

$$\text{Efficiency}_{\text{Red}_s} = 1 - \frac{\text{Red Targeting}(\text{red value})}{\text{Red} + \text{Yellow}(\text{red value})} \quad (12)$$

#### For red targeting in both

$$\text{Efficiency}_{\text{Red}_b} = 1 - \frac{\text{Both Targeting}(\text{red value})}{\text{Red} + \text{Yellow}(\text{red value})} \quad (13)$$

**Specificity.** Specificity provides insight into the system's ability to selectively target one gene without affecting the other. A high specificity indicates minimal off-target effects.

#### For Yellow Targeting:

$$\text{Specificity}_{\text{Yellow}_t} = \frac{\text{Yellow Targeting}(\text{red value})}{\text{Red} + \text{Yellow}(\text{red value})} \quad (14)$$



### For red targeting

$$\text{Specificity}_{\text{Red}_t} = \frac{\text{Red Targeting}(\text{yellow value})}{\text{Red} + \text{Yellow}(\text{yellow value})} \quad (15)$$

### Analysis CRISPRkit melanin production experiments

Melanin produced from tyrosinase tests exhibits a dark and black pigmentation, so no RGB extraction is required. Melanin expression analysis can be conducted with grayscale images and the expression values derived by comparing the brightness and darkness for each sample. Images taken of the experiment are first converted into grayscale and a single pixel value is extracted across each sample (*NC, PC, NG*...). This pixel value ranges from 0 to 255, with larger numbers representing a lighter shade. Then, the pixel value corresponding to each experimental sample is converted into expression values by subtracting it from the negative control *NC* value. Negative value treatment as described above is applied to all the expression values, and Prism 10 (GraphPad) is used for value plotting.

### High school data collection

All reagents were prepared in a laboratory setting, frozen in a  $-30\text{ }^{\circ}\text{C}$  freezer overnight, and transported to a local high school in a cardboard box on the morning when the tests were conducted. Reagents were not kept frozen during transport and were allowed to thaw gradually. The following was performed for two independent classes on the same day. Students were split into groups of 2-3 (each class contained around 20 students), and each group was given a CRISPRkit containing plasmid DNA, dCas9 protein, pre-aliquoted myTXTL Sigma 70 Master Mix, and 25 inoculation loops. Also distributed were the CRISPRkit protocols. Students were allowed as much time as they needed to complete the protocol, and all groups concluded by the end of 30 min. At least two instructors were present during the lab to answer questions. After the conclusion of both classes, kits were collected and incubated at  $28\text{ }^{\circ}\text{C}$  for 24 hrs. After 24 hrs, images were taken and used for CRISPRkit analysis.

On Day 2, kits were transported back to the local high school so that students could interpret their results, draw conclusions, and ask any final questions.

### Statistical analysis

For all one-way ANOVA tests, t-tests, and multiple comparison corrections, the level of significance ( $\alpha$ ) was set to 0.05. For each test, we assumed a Gaussian distribution of residuals and equal standard deviations for all conditions. The data generated by this study can be broadly classified into four categories, depending on the type of comparison made.

The first category consists of experiments that compared the expression levels of a single gene, encoding either a chromoprotein or fluorescent protein, under either a targeting sgRNA or no guide conditions using either Cas9 or dCas9 (Figs. 2c, d, 5a, 7e, Supplementary Fig. 3a). For each of these experiments, an unpaired two-tailed Student's t-test was used to compare the means of the fluorescence or absorbance values for the no guide and targeting sgRNA condition groups. P values calculated from these t-tests are displayed within each figure.

The second category consists of experiments which compared the differing expression levels of a single gene, encoding a chromoprotein, between targeting sgRNA and no-guide condition group pairs, which were paired according to another shared independent variable: incubation temperature or number of chromoprotein genes present (Figs. 3d, 4b). For each of these pairs, multiple unpaired two-tailed t-tests were used to compare the means of fluorescence values for each condition group within a pair. The Holm-Sidak test was then used to

correct for multiple comparisons between pairs within the same figure by calculating multiplicity-adjusted p values, which are displayed within each figure.

The third category consists of experiments that compared the expression levels of one or two genes under no-guide conditions to expression levels under single-guide and multiple-guide conditions (Figs. 3b, 4c, d, 5b, c, 6c, d, 7d, 8d, e, Supplementary Figs. 4a, 6b, 7b, 13b, c). For each of these genes, a one-way ordinary ANOVA was performed to compare the effect of chosen guide plasmid(s) on expression of the gene of interest. For figures containing dual-color chromoprotein data, a one-way ANOVA was performed for data for each chromoprotein gene. This ordinary one-way ANOVA test compared the means of fluorescence, absorbance, or CRISPRkit detection values of a no-guide or dual-color positive control condition group, single-guide condition groups, and multiple-guide condition groups. In all cases, the one-way ANOVA yielded a significant result, so Dunnett's multiple comparisons test was then performed to compare the means of the fluorescence, absorbance, or CRISPRkit detection values of single-guide condition groups and multi-guide condition groups to the means of the same values for no-guide condition groups, or to the dual-color positive control condition group if no-guide samples were not present. P values calculated from Dunnett's multiple comparisons test are displayed within each figure.

The fourth category consists of determining the correlation between our normalized plate-reader fluorescence or absorbance measurements and CRISPRkit output (Fig. 4f, Supplementary Fig. 3b, Supplementary Fig. 4b). We assumed the data was sampled from a Gaussian distribution and therefore performed a simple linear regression analysis.  $R^2$  is reported in each figure.

All statistical tests were conducted in Prism 10 (GraphPad). Summaries of fold changes and statistical tests are available in Supplementary Data 1 and Supplementary Data 2, respectively. All raw data used in statistical analysis are available in **Source Data**.

### Reporting summary

Further information on research design is available in the Nature Portfolio Reporting Summary linked to this article.

### Data availability

Source Data are provided with this paper. All plate reader and image analysis data generated in this study are provided in the Source Data file. The plasmids encoding the CRISPR kit will be available on Addgene: [https://www.addgene.org/Stanley\\_Qi/](https://www.addgene.org/Stanley_Qi/). The CRISPR kit can be requested from the CRISPR kit website at <https://www.crisprkit.org>. Source data are provided with this paper.

### Code availability

The code for data analysis is available via GitHub at <https://github.com/matthewbhla/crispr-kit/tree/main>.

### References

1. Jackson, S. S. et al. The accelerating pace of biotech democratization. *Nat. Biotechnol.* **37**, 1403–1408 (2019).
2. Beumer, K. Democratizing biotechnology requires more than availability. *Nat. Biotechnol.* **39**, 403 (2021).
3. Wang, J. Y. & Doudna, J. A. CRISPR technology: a decade of genome editing is only the beginning. *Science* **379**, eadd8643 (2023).
4. Horvath, P. & Barrangou, R. CRISPR/Cas, the immune system of bacteria and archaea. *Science* **327**, 167–170 (2010).
5. Wang, H., La Russa, M. & Qi, L. S. CRISPR/Cas9 in genome editing and beyond. *Annu Rev. Biochem* **85**, 227–264 (2016).
6. Frangoul, H. et al. CRISPR-Cas9 gene editing for sickle cell disease and  $\beta$ -thalassemia. *N. Engl. J. Med.* **384**, 252–260 (2021).



7. Dever, D. P. et al. CRISPR/Cas9  $\beta$ -globin gene targeting in human haematopoietic stem cells. *Nature* **539**, 384–389 (2016).
8. Zhu, H., Li, C. & Gao, C. Applications of CRISPR-Cas in agriculture and plant biotechnology. *Nat. Rev. Mol. Cell Biol.* **21**, 661–677 (2020).
9. Peters, J. M. et al. A comprehensive, CRISPR-based functional analysis of essential genes in bacteria. *Cell* **165**, 1493–1506 (2016).
10. Stark, J. C. et al. BioBits health: classroom activities exploring engineering, biology, and human health with fluorescent readouts. *ACS Synth. Biol.* **8**, 1001–1009 (2019).
11. Ziegler, H. & Nellen, W. CRISPR-Cas experiments for schools and the public. *Methods* **172**, 86–94 (2020).
12. McDonnell, L. et al. CRISPR in your kitchen: an At-Home CRISPR kit to edit genes in *Saccharomyces cerevisiae* used during a remote lab course. *J. Microbiol. Biol. Educ.* **23**, e00321-21 (2022).
13. Collias, D., Marshall, R., Collins, S. P., Beisel, C. L. & Noireaux, V. An educational module to explore CRISPR technologies with a cell-free transcription-translation system. *Synth. Biol. (Oxf.)* **4**, ysz005 (2019).
14. Mali, P. et al. RNA-guided human genome engineering via Cas9. *Science* **339**, 823–826 (2013).
15. Cong, L. et al. Multiplex genome engineering using CRISPR/Cas systems. *Science* **339**, 819–823 (2013).
16. Jinek, M. et al. A programmable dual-RNA-guided DNA endonuclease in adaptive bacterial immunity. *Science* **337**, 816–821 (2012).
17. Qi, L. S. et al. Repurposing CRISPR as an RNA-guided platform for sequence-specific control of gene expression. *Cell* **152**, 1173–1183 (2013).
18. Silverman, A. D., Karim, A. S. & Jewett, M. C. Cell-free gene expression: an expanded repertoire of applications. *Nat. Rev. Genet.* **21**, 151–170 (2020).
19. Huang, A. et al. BioBits™ explorer: a modular synthetic biology education kit. *Sci. Adv.* **4**, eaat5105 (2018).
20. Ahmed, F. H. et al. Over the rainbow: structural characterization of the chromoproteins gfasPurple, amilCP, spisPink and eforRed. *Acta Crystallogr D. Struct. Biol.* **78**, 599–612 (2022).
21. Liljeruhm, J. et al. Engineering a palette of eukaryotic chromoproteins for bacterial synthetic biology. *J. Biol. Eng.* **12**, 8 (2018).
22. Tamayo-Nuñez, J. et al. aeBlue chromoprotein color is temperature dependent. *Protein Pept. Lett.* **27**, 74–84 (2020).
23. Larson, M. H. et al. CRISPR interference (CRISPRi) for sequence-specific control of gene expression. *Nat. Protoc.* **8**, 2180–2196 (2013).
24. Liu, H. et al. CRISPR-ERA: a comprehensive design tool for CRISPR-mediated gene editing, repression and activation. *Bioinformatics* **31**, 3676–3678 (2015).
25. Rybnicky, G. A., Dixon, R. A., Kuhn, R. M., Karim, A. S. & Jewett, M. C. Development of a freeze-dried CRISPR-Cas12 sensor for detecting *wolbachia* in the secondary science classroom. *ACS Synth. Biol.* **11**, 835–842 (2022).
26. Alam, M. Z. et al. Melanin is a plenteous bioactive phenolic compound in date fruits (*Phoenix dactylifera* L.). *Sci. Rep.* **12**, 6614 (2022).
27. Liu, S. et al. Exploring the potential of water-soluble squid ink melanin: stability, free radical scavenging, and Cd<sup>2+</sup> adsorption abilities. *Foods* **12**, 3963 (2023).
28. Wang, X., Lu, D. & Tian, C. Analysis of melanin biosynthesis in the plant pathogenic fungus *Colletotrichum gloeosporioides*. *Fungal Biol.* **125**, 679–692 (2021).
29. Brenner, M. & Hearing, V. J. The protective role of melanin against UV damage in human skin. *Photochem Photobiol.* **84**, 539–549 (2008).
30. Hearing, V. J. & Jiménez, M. Mammalian tyrosinase—The critical regulatory control point in melanocyte pigmentation. *Int. J. Biochem.* **19**, 1141–1147 (1987).
31. Shuster, V. & Fishman, A. Isolation, cloning and characterization of a tyrosinase with improved activity in organic solvents from *Bacillus megaterium*. *J. Mol. Microbiol. Biotechnol.* **17**, 188–200 (2009).
32. Warfel, K. F. et al. A low-cost, thermostable, cell-free protein synthesis platform for on-demand production of conjugate vaccines. *ACS Synth. Biol.* **12**, 95–107 (2023).
33. Silverman, A. D., Kelley-Loughnane, N., Lucks, J. B. & Jewett, M. C. Deconstructing cell-free extract preparation for in vitro activation of transcriptional genetic circuitry. *ACS Synth. Biol.* **8**, 403–414 (2019).
34. della-Cioppa, G., Garger, S. J., Sverlow, G. G., Turpen, T. H. & Grill, L. K. Melanin production in *Escherichia coli* from a cloned tyrosinase gene. *Biotechnol. (N. Y.)* **8**, 634–638 (1990).
35. Fu, M. et al. Biosynthesis of melanin nanoparticles for photoacoustic imaging guided photothermal therapy. *Small* **19**, 2205343 (2023).

## Acknowledgements

The authors thank all members in the Lei Stanley Qi lab for helpful discussions. The authors thank Emily Ma for testing the CRISPRkit and providing valuable advice on improvement. The authors thank Dr. Huijun Zhou Ring and Daniel Stauber for helpful discussions. The authors thank Dr. Alex Engel and Dr. Phillip Kyriakakis for organizing undergraduate students at Stanford University for testing the CRISPRkit and offering helpful advice. The authors thank educators and high school teachers, including Meghan Strazicich, Temy Taylor, I-Heng McComb, and Johnson Huynh, for testing the kits and offering valuable advice. The authors thank James Stiltner, Jacob Russo, Tory Johnson, and their students at Los Altos High School, and Tanya Buxton and her students at Menlo School, for testing the CRISPRkit, and providing valuable feedback. The authors thank Dr. Peivand Sadat Mousavi for facilitating cell-free experiments. B.W. thanks the National Science Foundation Graduate Research Fellowship for support. S.C. thanks the Bio-X Bowes Graduate Student Fellowship for support. M.C.J. acknowledges support from the Army Research Office (W911NF-22-2-0210, W911NF-22-2-0246), the Department of Energy (DE-SC0023278), and the National Science Foundation (CBET – 1936789). L.S.Q. acknowledges support from the National Science Foundation CAREER award (no. 2046650), NIH Director's Pioneer Award DP1NS137219, National Institutes of Health (1R21AG077193, R21HG013133, R01CA266470), Bill & Melinda Gates Foundation (INV – 035661), and a gift from Chau Li Research Fund. L.S.Q. is a Chan Zuckerberg Biohub – San Francisco Investigator. The work is supported by the NSF CAREER award (no. 2046650) and the making@Stanford initiative (making.stanford.edu).

## Author contributions

M.B.L. and L.S.Q. conceived of the original idea. M.C., M.B.L., M.L.R. and L.S.Q. contributed significantly to the original frugal design. M.C., M.B.L., and M.L.R. cloned the chromoprotein plasmids and sgRNA plasmids. M.C. and M.B.L. performed the high-tech experiments. M.C. performed the low-tech experiments. M.B.L. developed the computational algorithm and the website. M.C. analyzed the experiments performed using laboratory equipment. M.B.L. analyzed experiments performed using smartphone images. W.M. and A.S. performed real-world tests. W.M. made significant improvements to the design. B.W. and M.J. assisted with in-house CFS and related experiments. S.C. contributed to the design and cloning of the melanin production plasmids. M.C., B.W., M.C.J., and L.S.Q. contributed to the design and implementation of the in-house CFS. M.C., M.B.L., and L.S.Q. plotted the figures. L.S.Q. and M.B.L. secured funding for the whole project and M.C.J. secured funding for in-house CFS preparation. L.S.Q. wrote the manuscript with significant edits from M.C. and M.B.L. and input from all authors.

## Competing interests

The authors declare no competing interests.

## Additional information

**Supplementary information** The online version contains supplementary material available at <https://doi.org/10.1038/s41467-024-50767-2>.

**Correspondence** and requests for materials should be addressed to Lei S. Qi.

**Peer review information** *Nature Communications* thanks Stephanie Lauer, and Claire Meaders for their contribution to the peer review of this work. A peer review file is available.

**Reprints and permissions information** is available at <http://www.nature.com/reprints>

**Publisher's note** Springer Nature remains neutral with regard to jurisdictional claims in published maps and institutional affiliations.

**Open Access** This article is licensed under a Creative Commons Attribution-NonCommercial-NoDerivatives 4.0 International License, which permits any non-commercial use, sharing, distribution and reproduction in any medium or format, as long as you give appropriate credit to the original author(s) and the source, provide a link to the Creative Commons licence, and indicate if you modified the licensed material. You do not have permission under this licence to share adapted material derived from this article or parts of it. The images or other third party material in this article are included in the article's Creative Commons licence, unless indicated otherwise in a credit line to the material. If material is not included in the article's Creative Commons licence and your intended use is not permitted by statutory regulation or exceeds the permitted use, you will need to obtain permission directly from the copyright holder. To view a copy of this licence, visit <http://creativecommons.org/licenses/by-nc-nd/4.0/>.

© The Author(s) 2024